Minimal lepton models with non-holomorphic modular A_4 symmetry*

Xiang-Yan Gao (高祥燕)[1,2,3†] Cai-Chang Li (黎才昌)[1,2,3‡]

[1]School of Physics, Northwest University, Xi'an 710127, China
[2]Shaanxi Key Laboratory for Theoretical Physics Frontiers, Xi'an 710127, China
[3]NSFC-SPTP Peng Huanwu Center for Fundamental Theory, Xi'an 710127, China

Abstract: We present a comprehensive bottom-up analysis of lepton mass and mixing based on the non-holomorphic A_4 modular symmetry. Neutrinos are assumed to be Majorana particles, and the light neutrino masses are generated through the Weinberg operator. In this framework, we construct all phenomenologically viable models with minimal number of free parameters, with the Yukawa couplings expressed in terms of polyharmonic Maaß forms of weights ±4, ±2, and 0 at level $N = 3$. Without imposing generalized CP (gCP) symmetry, we identify 147 (six) viable models with eight real free parameters that successfully reproduce the current experimental data of the lepton sector for the normal (inverted) mass ordering. When gCP symmetry consistent with A_4 modular symmetry is included, the number of free parameters is reduced by one, yielding 47 (five) phenomenologically viable models in the normal (inverted) mass ordering. Finally, we present detailed numerical analyses of a representative model for both mass orderings to illustrate these results.

Keywords: neutrino mixing, flavor symmetries, discrete symmetries, CP violation

DOI: 10.1088/1674-1137/ae3f0a **CSTR:** 32044.14.ChinesePhysicsC.50053109

I. INTRODUCTION

The Standard Model (SM) successfully describes particle interactions while failing to elucidate the origin of fermion families and their highly hierarchical masses and mixing patterns—a challenge known as the flavor problem [1]. The masses of fundamental particles span more than 12 orders of magnitude, ranging from the neutrino mass on the order of a fraction of an eV to the top quark mass of 173 GeV. Moreover, the quark mixing angles are small, whereas the lepton mixing angles include two large angles and one small angle comparable in magnitude to the Cabibbo angle [1]. The SM attributes these patterns to arbitrary Yukawa couplings, providing no underlying principle for their observed hierarchy and structure.

Several approaches have been developed to address the flavor problem. One framework introduces flavor symmetries, particularly non-Abelian discrete groups such as A_4, S_4 and A_5, which can naturally reproduce large lepton mixing [2−12]. In this framework, the spontaneous breaking of such a family symmetry by scalar flavon VEVs gives rise to the vacuum alignment problem, introducing additional complications. Modular invariance addresses these issues by offering an economical framework, in which Yukawa couplings are treated as modular forms transforming as irreducible representations of the finite modular groups Γ_N or Γ'_N. This approach eliminates flavons and the need for vacuum alignment [13−15], enabling the development of highly predictive fermion mass models. In the minimal modular invariant model, all lepton masses and mixing parameters are determined by only four real parameters along with the modulus τ [16, 17]. The same modulus can also link the quark and lepton sectors, allowing a simultaneous description of their flavor observables with only 14 real parameters, including the real and imaginary parts of τ [17, 18]. However, the predictive power of this framework is limited because modular symmetry only weakly constrains the Kähler potential [19]. Integrating modular symmetry with a traditional flavor symmetry mitigates this limitation and gives rise to either an eclectic flavor group [20−28] or quasi-eclectic flavor symmetry [29].

In the framework of the original modular invariance

Received 15 December 2025; Accepted 28 January 2026; Accepted manuscript online 29 January 2026

* Supported by Natural Science Basic Research Program of Shaanxi (2024JC-YBQN-0004) and the National Natural Science Foundation of China (12547106, 12247103)

† E-mail: 202421359@stumail.nwu.edu.cn

‡ E-mail: ccli@nwu.edu.cn

approach, the Yukawa couplings are assumed to be modular forms of level N, which are holomorphic functions of the complex modulus τ. To preserve this holomorphicity, supersymmetry (SUSY) is required [13, 30−32]. However, experimental evidence for low-energy SUSY remains elusive, making its natural realization uncertain. This lack of evidence motivates the study of non-supersymmetric modular invariant theories. Recently, a non-holomorphic modular flavor symmetry framework has been developed, which remains valid in non-supersymmetric settings [33]. In this framework, the holomorphicity condition is replaced by a harmonic one, and the Yukawa couplings are required to be polyharmonic Maaß forms of level N and even weight. These forms can be decomposed into multiplets of the inhomogeneous finite modular group Γ_N. Unlike holomorphic modular forms, which are defined only for non-negative weights $k \geq 0$, the polyharmonic Maaß forms extend to negative weights. Moreover, non-holomorphic polyharmonic Maaß exist for weights $k = 0, 1$, and 2. Phenomenologically viable models based on finite modular groups, such as $\Gamma_2 \cong S_3$ [34], $\Gamma_3 \cong A_4$ [33, 35−47], $\Gamma_4 \cong S_4$ [48], and $\Gamma_5 \cong A_5$ [49], have been successfully constructed. The framework has been further extended to include odd-weight polyharmonic Maaß forms, which transform under irreducible representations of the homogeneous finite modular groups Γ'_N [50]. Modular invariant models, based on the corresponding non-holomorphic groups $\Gamma'_3 \cong T'$ [50] and $\Gamma'_5 \cong A'_5$ [51], have also been studied. Furthermore, the non-holomorphic modular symmetry can consistently combine with generalized CP (gCP) symmetry, which restricts the phases of couplings, boosting modular invariant model predictions, similar to the phenomenon observed in supersymmetric modular flavor symmetry [52]. Under modular transformations, the gCP operation acts as $\tau \overset{\text{CP}}{\longmapsto} -\tau^*$ [20, 21, 52−54]. In the basis wherein S and T are unitary and symmetric across all irreducible representations, the gCP transformation simplifies to conventional CP, represented by the identity in flavor space.

This paper presents a systematic analysis of lepton models based on non-holomorphic A_4 modular symmetry. We focus on the most economical modular invariant constructions, which do not require any flavon field other than the modulus τ and generate light neutrino masses through the Weinberg operator. The three generations of left-handed leptons are assigned to the irreducible triplet representation **3** of A_4, whereas the right-handed leptons are allowed to transform as all possible combinations of the singlet representations **1**, **1′**, and **1″**. Using the level 3 polyharmonic Maaß forms of weights $k = \pm 4, \pm 2, 0$, we construct all phenomenologically viable and minimally parameterized lepton models. Without imposing gCP symmetry, 147 models for normal ordering (NO) and six models for inverted ordering (IO) successfully reproduce the experimental data. When gCP symmetry is enforced, 47 of the 147 NO models and five of the six IO models remain consistent with the observations in the lepton sector. The current JUNO [55] constraint on $\sin^2\theta_{12}$ rules out only five of the 147 viable NO models without gCP symmetry. All others remain consistent with current measurements. Notably, the non-holomorphic A_4 modular symmetry yields a richer set of level 3 polyharmonic Maaß forms than its supersymmetric framework [56]. This expanded landscape allows the construction of more viable minimal lepton models consistent with experimental data.

The rest of this paper is organized as follows. Section II presents a class of minimal lepton flavor models invariant under the non-holomorphic A_4 modular symmetry, and their predictions for lepton mixing angles, CP-violating phases, and neutrino masses are examined. A representative model is introduced in Section III, where a detailed numerical analysis is presented for both NO and IO neutrino mass spectra. Section IV presents the notable conclusions drawn from the findings of this study.

II. LEPTON MODELS BASED ON NON-HOLOMORPHIC A_4 MODULAR SYMMETRY

In this section, we systematically classify the minimal lepton mass models based on the finite modular symmetry $\Gamma_3 \cong A_4$ in the framework of non-SUSY. The Yukawa couplings are described by the polyharmonic Maaß forms of level $N = 3$ and even weights, which can be decomposed into the irreducible multiplets of A_4. The polyharmonic Maaß form multiplets of level 3 and weights ± 4, ± 2, and 0 are listed in Table 1. The explicit expressions for these forms are omitted here owing to their length and can be found in Ref. [33].

The finite modular group A_4 is generated by the modular transformations S and T, subject to the relations:

$$S^2 = (ST)^3 = T^3 = 1\,, \tag{1}$$

where the generators S and T in the three one-dimension-

Table 1. Polyharmonic Maaß form multiplets of level 3 and weights $k = \pm 4, \pm 2, 0$. The subscript $\boldsymbol{r}$ denotes the transformation property under the finite group A_4. The explicit forms of these polyharmonic Maaß form multiplets can be found in Ref. [33].

Weight k_Y	$k_Y = -4$	$k_Y = -2$	$k_Y = 0$	$k_Y = 2$	$k_Y = 4$
$Y_{\boldsymbol{r}}^{(k_Y)}$	$Y_{\boldsymbol{1}}^{(-4)}$, $Y_{\boldsymbol{3}}^{(-4)}$	$Y_{\boldsymbol{1}}^{(-2)}$, $Y_{\boldsymbol{3}}^{(-2)}$	$Y_{\boldsymbol{1}}^{(0)}$, $Y_{\boldsymbol{3}}^{(0)}$	$Y_{\boldsymbol{1}}^{(2)}$, $Y_{\boldsymbol{3}}^{(2)}$	$Y_{\boldsymbol{1}}^{(4)}$, $Y_{\boldsymbol{1'}}^{(4)}$, $Y_{\boldsymbol{3}}^{(4)}$

al irreducible representations **1**, **1′**, **1″** and one three-dimensional irreducible representation **3** are exporessed as

$$\begin{aligned}
&\mathbf{1}:\ S=1,\quad T=1,\\
&\mathbf{1}':\ S=1,\quad T=\omega,\\
&\mathbf{1}'':\ S=1,\quad T=\omega^2,\\
&\mathbf{3}:\ S=\frac{1}{3}\begin{pmatrix}-1&2&2\\2&-1&2\\2&2&-1\end{pmatrix},\quad T=\begin{pmatrix}1&0&0\\0&\omega&0\\0&0&\omega^2\end{pmatrix},
\end{aligned}\tag{2}$$

with $\omega=\mathrm{e}^{2\pi\mathrm{i}/3}$. For any two triplet $x=(x_1,x_2,x_3)$ and $y=(y_1,y_2,y_3)$, the tensor product decomposition $\mathbf{3}\otimes\mathbf{3}=\mathbf{1}\oplus\mathbf{1}'\oplus\mathbf{1}''\oplus\mathbf{3}_S\oplus\mathbf{3}_A$ is given by [57]

$$\begin{aligned}
(xy)_{\mathbf{1}}&=x_1y_1+x_2y_3+x_3y_2,\\
(xy)_{\mathbf{1}'}&=x_3y_3+x_1y_2+x_2y_1,\\
(xy)_{\mathbf{1}''}&=x_2y_2+x_1y_3+x_3y_1,\\
(xy)_{\mathbf{3}_S}&=(2x_1y_1-x_2y_3-x_3y_2,2x_3y_3-x_1y_2-x_2y_1,\\
&\quad 2x_2y_2-x_1y_3-x_3y_1),\\
(xy)_{\mathbf{3}_A}&=(x_2y_3-x_3y_2,x_1y_2-x_2y_1,x_3y_1-x_1y_3).
\end{aligned}\tag{3}$$

where $\mathbf{3}_S$ and $\mathbf{3}_A$ refer to the symmetric and antisymmetric combinations, respectively. In our working basis, T is diagonal, and S is real and symmetric in all A_4 irreducible representations. Consequently, because of the gCP invariance, the coupling constants accompanying each invariant singlet in the Lagrangian are real.

In the present study, neutrinos are assumed to be Majorana particles, and the light neutrino masses are generated via the Weinberg operator. The analysis focuses on the most economical scenarios, in which modular invariance is attained without introducing any flavon field other than the complex modulus τ. We assume that the Higgs doublet fields H have vanishing modular weight and transform as the trivial singlet **1** of A_4. The left-handed (LH) lepton doublets L, with a modular weight k_L, form a triplet **3**, whereas the three right-handed (RH) charged leptons $E^c_{1,2,3}$ are A_4 singlets with modular weights $k_{E^c_{1,2,3}}$. To minimize the number of free parameters, we restrict the analysis to polyharmonic Maaß forms of level 3 with even weights ranging from $k=-4$ to 4, prioritizing the use of the lowest weight forms whenever possible.

A. Charged lepton sector

We identify 10 distinct independent representation assignments for the lepton fields, with the LH doublets forming a triplet, and the RH charged leptons appearing as singlets. Among these, three assignments feature all three RH leptons transforming under the same singlet, six assignments have two RH leptons transforming under one singlet and the third RH lepton under another singlet, and one assignment has all three RH leptons transforming under distinct singlets. Therefore, the charged lepton sector is divided into 10 different cases, labeled $C_1^{(k_1,k_2,k_3)}$ to $C_{10}^{(k_1,k_2,k_3)}$, with the corresponding representation assignments summarized in Table 2. For all the 10 assignments, the most general Lagrangian $\mathcal{L}_e$ describing the charged lepton masses is

$$\begin{aligned}
C_1^{(k_1,k_2,k_3)}&:-\mathcal{L}_e=[\alpha E_1^c\left(LY_{\mathbf{3}}^{(k_1)}\right)_{\mathbf{1}}+\beta E_2^c\left(LY_{\mathbf{3}}^{(k_2)}\right)_{\mathbf{1}}\\
&\quad+\gamma E_3^c\left(LY_{\mathbf{3}}^{(k_3)}\right)_{\mathbf{1}}]H^*,\\
C_2^{(k_1,k_2,k_3)}&:-\mathcal{L}_e=[\alpha E_1^c\left(LY_{\mathbf{3}}^{(k_1)}\right)_{\mathbf{1}''}+\beta E_2^c\left(LY_{\mathbf{3}}^{(k_2)}\right)_{\mathbf{1}''}\\
&\quad+\gamma E_3^c\left(LY_{\mathbf{3}}^{(k_3)}\right)_{\mathbf{1}''}]H^*,\\
C_3^{(k_1,k_2,k_3)}&:-\mathcal{L}_e=[\alpha E_1^c\left(LY_{\mathbf{3}}^{(k_1)}\right)_{\mathbf{1}'}+\beta E_2^c\left(LY_{\mathbf{3}}^{(k_2)}\right)_{\mathbf{1}'}\\
&\quad+\gamma E_3^c\left(LY_{\mathbf{3}}^{(k_3)}\right)_{\mathbf{1}'}]H^*,\\
C_4^{(k_1,k_2,k_3)}&:-\mathcal{L}_e=[\alpha E_1^c\left(LY_{\mathbf{3}}^{(k_1)}\right)_{\mathbf{1}}+\beta E_2^c\left(LY_{\mathbf{3}}^{(k_2)}\right)_{\mathbf{1}}\\
&\quad+\gamma E_3^c\left(LY_{\mathbf{3}}^{(k_3)}\right)_{\mathbf{1}''}]H^*,\\
C_5^{(k_1,k_2,k_3)}&:-\mathcal{L}_e=[\alpha E_1^c\left(LY_{\mathbf{3}}^{(k_1)}\right)_{\mathbf{1}}+\beta E_2^c\left(LY_{\mathbf{3}}^{(k_2)}\right)_{\mathbf{1}}\\
&\quad+\gamma E_3^c\left(LY_{\mathbf{3}}^{(k_3)}\right)_{\mathbf{1}'}]H^*,\\
C_6^{(k_1,k_2,k_3)}&:-\mathcal{L}_e=[\alpha E_1^c\left(LY_{\mathbf{3}}^{(k_1)}\right)_{\mathbf{1}''}+\beta E_2^c\left(LY_{\mathbf{3}}^{(k_2)}\right)_{\mathbf{1}''}\\
&\quad+\gamma E_3^c\left(LY_{\mathbf{3}}^{(k_3)}\right)_{\mathbf{1}}]H^*,\\
C_7^{(k_1,k_2,k_3)}&:-\mathcal{L}_e=[\alpha E_1^c\left(LY_{\mathbf{3}}^{(k_1)}\right)_{\mathbf{1}''}+\beta E_2^c\left(LY_{\mathbf{3}}^{(k_2)}\right)_{\mathbf{1}''}\\
&\quad+\gamma E_3^c\left(LY_{\mathbf{3}}^{(k_3)}\right)_{\mathbf{1}'}]H^*,\\
C_8^{(k_1,k_2,k_3)}&:-\mathcal{L}_e=[\alpha E_1^c\left(LY_{\mathbf{3}}^{(k_1)}\right)_{\mathbf{1}'}+\beta E_2^c\left(LY_{\mathbf{3}}^{(k_2)}\right)_{\mathbf{1}'}\\
&\quad+\gamma E_3^c\left(LY_{\mathbf{3}}^{(k_3)}\right)_{\mathbf{1}}]H^*,\\
C_9^{(k_1,k_2,k_3)}&:-\mathcal{L}_e=[\alpha E_1^c\left(LY_{\mathbf{3}}^{(k_1)}\right)_{\mathbf{1}'}+\beta E_2^c\left(LY_{\mathbf{3}}^{(k_2)}\right)_{\mathbf{1}'}\\
&\quad+\gamma E_3^c\left(LY_{\mathbf{3}}^{(k_3)}\right)_{\mathbf{1}''}]H^*,\\
C_{10}^{(k_1,k_2,k_3)}&:-\mathcal{L}_e=[\alpha E_1^c\left(LY_{\mathbf{3}}^{(k_1)}\right)_{\mathbf{1}}+\beta E_2^c\left(LY_{\mathbf{3}}^{(k_2)}\right)_{\mathbf{1}''}\\
&\quad+\gamma E_3^c\left(LY_{\mathbf{3}}^{(k_3)}\right)_{\mathbf{1}'}]H^*,
\end{aligned}\tag{4}$$

where the weights of polyharmonic Maaß form triplets $Y_{\mathbf{3}}^{(k_i)}$ satisfy $k_i=k_L+k_{E_i^c}$ $(i=1,2,3)$, and the phases of the couplings α, β, and γ can be fully absorbed by rephasing the RH charged lepton fields E_1^c, E_2^c, and E_3^c, respectively. Consequently, these couplings can be taken as real and positive.

In each of the first three cases in Eq. (4), all three RH charged leptons E_i^c transform under the same A_4 singlet representation. They are distinguished by their modular weights $k_{E_i^c}$, which are achieved by coupling each to

Table 2. Possible assignments for the A_4 representations and modular weights of the lepton fields. The LH doublets L form a triplet **3** under A_4 with a modular weight k_L. The RH charged leptons E_i^c $(i=1,2,3)$ transform under A_4 as $\rho_{E_i^c}$ with modular weights $k_{E_i^c}$. The polyharmonic Maaß form triplet $Y_{\mathbf{3}}^{(k_i)}$ satisfies $k_i = k_L + k_{E_i^c}$, and $v = \langle H \rangle$ denotes the vacuum expectation value of the Higgs field.

Cases	$(\rho_{E_1^c}, \rho_{E_2^c}, \rho_{E_3^c})$	(k_1, k_2, k_3)	M_e
$C_1^{(k_1,k_2,k_3)}$	$(\mathbf{1},\mathbf{1},\mathbf{1})$	$k_1 < k_2 < k_3 \in \{\pm4, \pm2, 0\}$	$\begin{pmatrix} \alpha Y_{\mathbf{3},1}^{(k_1)} & \alpha Y_{\mathbf{3},3}^{(k_1)} & \alpha Y_{\mathbf{3},2}^{(k_1)} \\ \beta Y_{\mathbf{3},1}^{(k_2)} & \beta Y_{\mathbf{3},3}^{(k_2)} & \beta Y_{\mathbf{3},2}^{(k_2)} \\ \gamma Y_{\mathbf{3},1}^{(k_3)} & \gamma Y_{\mathbf{3},3}^{(k_2)} & \gamma Y_{\mathbf{3},2}^{(k_3)} \end{pmatrix} v$
$C_2^{(k_1,k_2,k_3)}$	$(\mathbf{1}',\mathbf{1}',\mathbf{1}')$		$\begin{pmatrix} \alpha Y_{\mathbf{3},3}^{(k_1)} & \alpha Y_{\mathbf{3},2}^{(k_1)} & \alpha Y_{\mathbf{3},1}^{(k_1)} \\ \beta Y_{\mathbf{3},3}^{(k_2)} & \beta Y_{\mathbf{3},2}^{(k_2)} & \beta Y_{\mathbf{3},1}^{(k_2)} \\ \gamma Y_{\mathbf{3},3}^{(k_3)} & \gamma Y_{\mathbf{3},2}^{(k_3)} & \gamma Y_{\mathbf{3},1}^{(k_3)} \end{pmatrix} v$
$C_3^{(k_1,k_2,k_3)}$	$(\mathbf{1}'',\mathbf{1}'',\mathbf{1}'')$		$\begin{pmatrix} \alpha Y_{\mathbf{3},2}^{(k_1)} & \alpha Y_{\mathbf{3},1}^{(k_1)} & \alpha Y_{\mathbf{3},3}^{(k_1)} \\ \beta Y_{\mathbf{3},2}^{(k_2)} & \beta Y_{\mathbf{3},1}^{(k_2)} & \beta Y_{\mathbf{3},3}^{(k_2)} \\ \gamma Y_{\mathbf{3},2}^{(k_3)} & \gamma Y_{\mathbf{3},1}^{(k_3)} & \gamma Y_{\mathbf{3},3}^{(k_3)} \end{pmatrix} v$
$C_4^{(k_1,k_2,k_3)}$	$(\mathbf{1},\mathbf{1},\mathbf{1}')$	$k_1 < k_2 \in \{\pm4, \pm2, 0\}$, $k_3 \in \{\pm4, \pm2, 0\}$	$\begin{pmatrix} \alpha Y_{\mathbf{3},1}^{(k_1)} & \alpha Y_{\mathbf{3},3}^{(k_1)} & \alpha Y_{\mathbf{3},2}^{(k_1)} \\ \beta Y_{\mathbf{3},1}^{(k_2)} & \beta Y_{\mathbf{3},3}^{(k_2)} & \beta Y_{\mathbf{3},2}^{(k_2)} \\ \gamma Y_{\mathbf{3},3}^{(k_3)} & \gamma Y_{\mathbf{3},2}^{(k_3)} & \gamma Y_{\mathbf{3},1}^{(k_3)} \end{pmatrix} v$
$C_5^{(k_1,k_2,k_3)}$	$(\mathbf{1},\mathbf{1},\mathbf{1}'')$		$\begin{pmatrix} \alpha Y_{\mathbf{3},1}^{(k_1)} & \alpha Y_{\mathbf{3},3}^{(k_1)} & \alpha Y_{\mathbf{3},2}^{(k_1)} \\ \beta Y_{\mathbf{3},1}^{(k_2)} & \beta Y_{\mathbf{3},3}^{(k_2)} & \beta Y_{\mathbf{3},2}^{(k_2)} \\ \gamma Y_{\mathbf{3},2}^{(k_3)} & \gamma Y_{\mathbf{3},1}^{(k_3)} & \gamma Y_{\mathbf{3},3}^{(k_3)} \end{pmatrix} v$
$C_6^{(k_1,k_2,k_3)}$	$(\mathbf{1}',\mathbf{1}',\mathbf{1})$		$\begin{pmatrix} \alpha Y_{\mathbf{3},3}^{(k_1)} & \alpha Y_{\mathbf{3},2}^{(k_1)} & \alpha Y_{\mathbf{3},1}^{(k_1)} \\ \beta Y_{\mathbf{3},3}^{(k_2)} & \beta Y_{\mathbf{3},2}^{(k_2)} & \beta Y_{\mathbf{3},1}^{(k_2)} \\ \gamma Y_{\mathbf{3},1}^{(k_3)} & \gamma Y_{\mathbf{3},3}^{(k_3)} & \gamma Y_{\mathbf{3},2}^{(k_3)} \end{pmatrix} v$
$C_7^{(k_1,k_2,k_3)}$	$(\mathbf{1}',\mathbf{1}',\mathbf{1}'')$		$\begin{pmatrix} \alpha Y_{\mathbf{3},3}^{(k_1)} & \alpha Y_{\mathbf{3},2}^{(k_1)} & \alpha Y_{\mathbf{3},1}^{(k_1)} \\ \beta Y_{\mathbf{3},3}^{(k_2)} & \beta Y_{\mathbf{3},2}^{(k_2)} & \beta Y_{\mathbf{3},1}^{(k_2)} \\ \gamma Y_{\mathbf{3},2}^{(k_3)} & \gamma Y_{\mathbf{3},1}^{(k_3)} & \gamma Y_{\mathbf{3},3}^{(k_3)} \end{pmatrix} v$
$C_8^{(k_1,k_2,k_3)}$	$(\mathbf{1}'',\mathbf{1}'',\mathbf{1})$		$\begin{pmatrix} \alpha Y_{\mathbf{3},2}^{(k_1)} & \alpha Y_{\mathbf{3},1}^{(k_1)} & \alpha Y_{\mathbf{3},3}^{(k_1)} \\ \beta Y_{\mathbf{3},2}^{(k_2)} & \beta Y_{\mathbf{3},1}^{(k_2)} & \beta Y_{\mathbf{3},3}^{(k_2)} \\ \gamma Y_{\mathbf{3},1}^{(k_3)} & \gamma Y_{\mathbf{3},3}^{(k_3)} & \gamma Y_{\mathbf{3},2}^{(k_3)} \end{pmatrix} v$
$C_9^{(k_1,k_2,k_3)}$	$(\mathbf{1}'',\mathbf{1}'',\mathbf{1}')$		$\begin{pmatrix} \alpha Y_{\mathbf{3},2}^{(k_1)} & \alpha Y_{\mathbf{3},1}^{(k_1)} & \alpha Y_{\mathbf{3},3}^{(k_1)} \\ \beta Y_{\mathbf{3},2}^{(k_2)} & \beta Y_{\mathbf{3},1}^{(k_2)} & \beta Y_{\mathbf{3},3}^{(k_2)} \\ \gamma Y_{\mathbf{3},3}^{(k_3)} & \gamma Y_{\mathbf{3},2}^{(k_3)} & \gamma Y_{\mathbf{3},1}^{(k_3)} \end{pmatrix} v$
$C_{10}^{(k_1,k_2,k_3)}$	$(\mathbf{1},\mathbf{1}',\mathbf{1}'')$	$k_1, k_2, k_3 \in \{\pm4, \pm2, 0\}$	$\begin{pmatrix} \alpha Y_{\mathbf{3},1}^{(k_1)} & \alpha Y_{\mathbf{3},3}^{(k_1)} & \alpha Y_{\mathbf{3},2}^{(k_1)} \\ \beta Y_{\mathbf{3},3}^{(k_2)} & \beta Y_{\mathbf{3},2}^{(k_2)} & \beta Y_{\mathbf{3},1}^{(k_2)} \\ \gamma Y_{\mathbf{3},2}^{(k_3)} & \gamma Y_{\mathbf{3},1}^{(k_3)} & \gamma Y_{\mathbf{3},3}^{(k_3)} \end{pmatrix} v$

modular form multiplets of different weights. In this study, the charged lepton mass matrix M_e is defined by the convention $E^c M_e L$. Permuting any two rows of M_e corresponds to a field redefinition of the corresponding RH leptons, and consequently, the predictions for masses and mixing parameters remain unchanged. Similarly, exchanging the modular weights of any two RH charged lepton fields also yields identical physical predictions. For minimality and simplicity, we assume $k_1 < k_2 < k_3 \in \{\pm4, \pm2, 0\}$ without loss of generality, which results in 10 distinct charged lepton mass matrices from the 10 independent weight assignments in each of the three cases. The corresponding lepton mass matrices are summarized in Table 2.

For the six cases $C_4^{(k_1,k_2,k_3)}$ to $C_9^{(k_1,k_2,k_3)}$, two RH charged leptons are assigned to one A_4 singlet, whereas the third lepton is assigned to a different singlet. Without loss of generality, we assume that E_1^c and E_2^c transform under the same singlet, whereas E_3^c transforms under another singlet. This transformation leads to 50 independent weight assignments for each of the six cases, obtained from the combinations satisfying $k_1 < k_2 \in \{\pm4, \pm2, 0\}$ and $k_3 \in \{\pm4, \pm2, 0\}$. The corresponding representation assignments to RH charged lepton fields, along with the charged lepton mass matrices, are presented Table 2.

In the final case $C_{10}^{(k_1,k_2,k_3)}$, the three RH charged leptons E_i^c are assigned to the three distinct A_4 singlets **1**, **1**′, and **1**″. Their modular weights may be identical. For minimality and simplicity, the weights $k_i = k_L + k_{E_i^c}$ are selected from the set $\pm4, \pm2, 0$, resulting in a total of 125 possible weight assignments for k_i. The charged lepton mass matrix for each weight assignment is given in Table 2.

B. Neutrino sector

In the present study, the neutrinos are assumed to be Majorana particles, and their masses are described by the effective Weinberg operator. According to the symmetry constraints of the model, when the LH lepton doublets L transform as triplet **3** under A_4, the antisymmetric combination $(LL)_{\mathbf{3}_A}$ vanishes. Therefore, non-zero neutrino masses require either a singlet polyharmonic Maaß form $Y_{\mathbf{1}}^{(2k_L)}$, $Y_{\mathbf{1}'}^{(2k_L)}$, $Y_{\mathbf{1}''}^{(2k_L)}$ or a triplet polyharmonic Maaß form $Y_{\mathbf{3}}^{(2k_L)}$. Then, the most general modular invariant Lagrangian for neutrino masses can be written as

$$W_j : -\mathcal{L}_\nu = \frac{H^2}{2\Lambda}\left[g_1 Y_{\mathbf{1}}^{(k_j)}(LL)_{\mathbf{1}} + g_2\left((LL)_{\mathbf{3_S}} Y_{\mathbf{3}}^{(k_j)}\right)_{\mathbf{1}} + g_3 Y_{\mathbf{1}'}^{(k_j)}(LL)_{\mathbf{1}''} + g_4 Y_{\mathbf{1}''}^{(k_j)}(LL)_{\mathbf{1}'}\right]. \tag{5}$$

where for simplicity, we consider four distinct cases W_j $(j=1,2,3,4)$ corresponding to the modular weights $k_j = 2k_L = -4,-2,0,2$, respectively. In these four cases, the last two terms in Eq. (5) vanish because of the absence of corresponding polyharmonic Maaß forms $Y_{\mathbf{1}'}^{(k_j)}$ and $Y_{\mathbf{1}''}^{(k_j)}$ at these weights. Consequently, the resulting light neutrino mass matrix depends only on the two parameters g_1 and g_2. Applying the decomposition rule of the finite modular group A_4, the light neutrino mass matrix can be written in the following form:

$$M_\nu(k_j) = \frac{v^2}{2\Lambda}\begin{pmatrix} g_1 Y_{\mathbf{1}}^{(k_j)} + 2g_2 Y_{\mathbf{3},1}^{(k_j)} & -g_2 Y_{\mathbf{3},3}^{(k_j)} & -g_2 Y_{\mathbf{3},2}^{(k_j)} \\ -g_2 Y_{\mathbf{3},3}^{(k_j)} & 2g_2 Y_{\mathbf{3},2}^{(k_j)} & g_1 Y_{\mathbf{1}}^{(k_j)} - g_2 Y_{\mathbf{3},1}^{(k_j)} \\ -g_2 Y_{\mathbf{3},2}^{(k_j)} & g_1 Y_{\mathbf{1}}^{(k_j)} - g_2 Y_{\mathbf{3},1}^{(k_j)} & 2g_2 Y_{\mathbf{3},3}^{(k_j)} \end{pmatrix}, \tag{6}$$

where the phase of g_1 can be eliminated by field redefinition, whereas that of g_2 remains physical and cannot be removed. In our working basis, both g_1 and g_2 are real under gCP symmetry.

C. Numerical results

In Sections II.A and II.B, we have separately discussed the representation, weight assignments, and resulting mass matrices for the charged leptons and neutrinos, respectively. We assume that the LH doublet leptons transform as the A_4 triplet **3**, whereas the RH charged leptons are assigned to A_4 singlets. Considering the 10 possible representation assignments for the RH charged lepton fields and polyharmonic Maaß form multiplets $Y_{\mathbf{r}}^{(k)}$ within the modular weight range $-4 \le k \le 4$, we observe that 455 specific assignments lead to charged lepton mass matrices that can be described by only three real parameters. The corresponding representation and weight assignments, along with all such mass matrices, are summarized in Table 2. In the charged lepton sector, k_L is relatively unconstrained, whereas the sum $k_i = k_{E_i^c} + k_L$ is fixed as shown in this table. Neutrino masses are generated via the effective Weinberg operator. Corresponding to the weight k_L, only four distinct assignments yield light neutrino mass matrices described by the minimal set of free parameters. The corresponding mass matrices are given in Eq. (6).

When constructing explicit lepton models, the representation and modular weight assignments of the lepton doublet L must be selected consistently in both the charged lepton and neutrino sectors. As explained before, we assume that the left-handed leptons transform as the A_4 triplet **3** in both the sectors. Combining the possible structures from the charged lepton mass matrices in Table 2 and the neutrino mass matrices in Eq. (6) yields a total of $455\times 4 = 1820$ minimal non-supersymmetric lepton models based on the finite modular group A_4. These models are labeled as $\{C_m^{(k_1,k_2,k_3)}, W_j\}$, where $m = 1,2,\ldots,10$ and $j = 1,2,3,4$. For each model, the modular weights of the matter fields are uniquely determined, although their explicit values are not listed here. Notably, the coupling constants α, β, and γ in the charged lepton mass matrices can be chosen as positive real numbers. The light neutrino mass matrices contain two additional real parameters $|g_2/g_1|$ and $\arg(g_2/g_1)$ in addition to the overall factor $g_1 v^2/\Lambda$ and modulus τ. Thus, in the absence of gCP symmetry, all 1820 models involve eight independent real parameters. When gCP symmetry compatible with A_4 is imposed, the ratio g_2/g_1 is further constrained to be real, reducing the number of real input parameters to seven.

For each lepton flavor model, we must verify its ability to reproduce the experimental data within uncertainties. Accordingly, we perform systematic numerical and χ^2 analyses of all the 1820 minimal lepton models with and without gCP symmetry and for both NO and IO neutrino mass spectra. The χ^2 function is defined in the following standard form:

$$\chi^2 = \sum_{i=1}^{7}\left(\frac{P_i(x) - O_i}{\sigma_i}\right)^2, \tag{7}$$

where O_i and σ_i denote the central values and 1σ uncertainties of the seven dimensionless observables, respectively,

$$m_e/m_\mu,\quad m_\mu/m_\tau,\quad \sin^2\theta_{12},\quad \sin^2\theta_{13},\quad \sin^2\theta_{23},\quad \delta_{\rm CP},\quad \Delta m^2_{21}/\Delta m^2_{3l}, \tag{8}$$

as listed in Table 3. Here, the lepton mixing parameters are adopted from NuFIT 6.0 with inclusion of the data on atmospheric neutrinos provided by the Super-Kami-

Table 3. Best fit values; 1σ and 3σ ranges for the mixing parameters and lepton mass ratios are presented The experimental data and uncertainties for both the NO and IO neutrino mass spectra are sourced from NuFIT 6.0 with Super-Kamiokande atmospheric data [58]. Notably, $\Delta m^2_{3\ell} = \Delta m^2_{31} > 0$ for NO and $\Delta m^2_{3\ell} = \Delta m^2_{32} < 0$ for IO. The 1σ uncertainties for the charged lepton mass ratios are considered to be 0.1% of their central values in the χ^2 analysis.

Observables	NO		IO	
	bf $\pm 1\sigma$	3σ region	bf $\pm 1\sigma$	3σ region
$\sin^2\theta_{13}$	$0.02215^{+0.00056}_{-0.00058}$	[0.02030, 0.02388]	$0.02231^{+0.00056}_{-0.00056}$	[0.02060, 0.02409]
$\sin^2\theta_{12}$	$0.308^{+0.012}_{-0.011}$	[0.275, 0.345]	$0.308^{+0.012}_{-0.011}$	[0.275, 0.345]
$\sin^2\theta_{23}$	$0.470^{+0.017}_{-0.013}$	[0.435, 0.585]	$0.550^{+0.012}_{-0.015}$	[0.440, 0.584]
$\delta_{\rm CP}/\pi$	$1.178^{+0.144}_{-0.228}$	[0.689, 2.022]	$1.522^{+0.122}_{-0.139}$	[1.117, 1.861]
$\frac{\Delta m^2_{21}}{10^{-5}\text{eV}^2}$	$7.49^{+0.19}_{-0.19}$	[6.92, 8.05]	$7.49^{+0.19}_{-0.19}$	[6.92, 8.05]
$\frac{\Delta m^2_{3\ell}}{10^{-3}\text{eV}^2}$	$2.513^{+0.021}_{-0.019}$	[2.451, 2.578]	$-2.484^{+0.020}_{-0.020}$	[−2.547, −2.421]
$\Delta m^2_{21}/\Delta m^2_{3\ell}$	$0.0298^{+0.00079}_{-0.00079}$	[0.0268, 0.0328]	$-0.0302^{+0.00080}_{-0.00080}$	[−0.0333, −0.0272]
m_e/m_μ	0.004737	—	0.004737	—
m_μ/m_τ	0.05882	—	0.05882	—
m_e/MeV	0.469652	—	0.469652	—

okande [58]. $P_i(x)$ in Eq. (7) represents the model predictions for these observables for a given set of input parameters x. When gCP symmetry is not imposed, x consists of the following six parameters:

$$\Re\tau, \quad \Im\tau, \quad \beta/\alpha, \quad \gamma/\alpha, \quad |g_2/g_1|, \quad \text{Arg}(g_2/g_1). \tag{9}$$

If gCP symmetry is included, then $\text{Arg}(g_2/g_1)$ is restricted to 0 or π, reducing the number of free parameters to five. In this study, the absolute values of the Yukawa coupling ratios are uniformly sampled in $[0, 10^6]$, and the phase $\text{Arg}(g_2/g_1)$ is sampled in $[0, 2\pi)$. The complex modulus τ is restricted to lie in the fundamental domain $\mathcal{D} = \left\{\tau \in \mathcal{H} \middle| -\frac{1}{2} \le \Re(\tau) \le \frac{1}{2}, |\tau| \ge 1\right\}$, because the underlying theory has the modular symmetry $\bar{\Gamma}$, and consequently, vacua related by modular transformations are physically equivalent [59]. Notably, the overall parameter αv of the charged lepton mass matrix and the normalization factor $g_1 v^2/\Lambda$ of the light neutrino mass matrix can be determined by the experimentally measured electron mass m_e and solar neutrino mass squared difference Δm^2_{21}, respectively.

For each set of input parameters, we can calculate the corresponding predictions for lepton masses, mixing parameters, χ^2 function, as well as the effective mass $m_{\beta\beta}$ in neutrinoless double beta decay ($0\nu\beta\beta$-decay) and the kinematical mass m_β in beta decay which are defined as:

$$m_{\beta\beta} = \left|\sum_i^3 m_i U_{1i}^2\right|, \qquad m_\beta = \left[\sum_i^3 m_i^2 |U_{1i}|^2\right]^{1/2}, \tag{10}$$

where m_i are the light neutrino masses and U is the PMNS matrix. We adopt the standard parametrization of the PMNS matrix [1]:

$$U = \begin{pmatrix} c_{12}c_{13} & s_{12}c_{13} & s_{13}e^{-i\delta_{\rm CP}} \\ -s_{12}c_{23} - c_{12}s_{13}s_{23}e^{i\delta_{\rm CP}} & c_{12}c_{23} - s_{12}s_{13}s_{23}e^{i\delta_{\rm CP}} & c_{13}s_{23} \\ s_{12}s_{23} - c_{12}s_{13}c_{23}e^{i\delta_{\rm CP}} & -c_{12}s_{23} - s_{12}s_{13}c_{23}e^{i\delta_{\rm CP}} & c_{13}c_{23} \end{pmatrix} \text{diag}(1, e^{i\frac{\alpha_{21}}{2}}, e^{i\frac{\alpha_{31}}{2}}), \tag{11}$$

where $c_{ij} \equiv \cos\theta_{ij}$, $s_{ij} \equiv \sin\theta_{ij}$, $\delta_{\rm CP}$ is the Dirac CP-violating phase, and $\alpha_{21,31}$ are Majorana CP-violating phases [60].

Next, we compare the predictions of the 1820 models with the latest NuFIT results. A model is phenomenologically viable if its predicted lepton mass ratios and mixing parameters at the χ^2 minimum fall within the 3σ intervals provided in Table 3. Furthermore, in our analysis, we select models whose predictions must also satisfy the constraint that the total neutrino mass $\sum_{i=1}^3 m_i$ must be below the Planck + lensing + BAO limit of 120 meV [61]. Through comprehensive scanning of the input parameter

space, we systematically determine the minimal χ^2 values. The analysis of the 1820 models without gCP symmetry reveals that 147 are compatible with experimental data in the NO mass spectrum, whereas only six are compatible in the IO. The complete fitting results for these viable models, including the input parameters, mixing angles, CP-violating phases, neutrino masses, effective mass $m_{\beta\beta}$ in $0\nu\beta\beta$-decay, and kinematical mass m_β in beta decay are summarized in Table 4 and Table 6. When the finite modular group is extended to include gCP symmetry, only 47 out of the 147 models for NO and five out of the six model for IO produce results compatible with the experimental data of lepton mixing parameters and masses. The best fit values of the input parameters, mixing parameters and lepton masses are presented in Table 5 and Table 7. Evidently, five models without gCP symmetry and in the NO case —namely $\{C_2^{(-2,0,2)}, W_1\}$, $\{C_2^{(-2,0,4)}, W_1\}$, $\{C_6^{(-2,0,-2)}, W_1\}$, $\{C_6^{(-2,0,0)}, W_1\}$ and $\{C_7^{(-4,4,-4)}, W_1\}$—are disfavored once the current JUNO 59.1-day constraint on $\sin^2\theta_{12}$ is applied [55]. Their predicted values lie within the 3σ interval

$$0.2831 \leq \sin^2\theta_{12} \leq 0.3353\,, \tag{12}$$

which is derived from the central value $\sin^2\theta_{12} = 0.3092 \pm 0.0087$ by subtracting three times the 1σ uncertainty. All remaining models remain compatible with current oscillation data, including this JUNO measurement. Note that the Weinberg operator model discussed in Ref.

Table 4. Best fit values of the input parameters, three mixing angles θ_{12}, θ_{13}, θ_{23}, Dirac CP-violating phase $\delta_{\rm CP}$, Majorana CP-violating phases α_{21}, α_{31}, three light neutrino masses $m_{1,2,3}$, the effective mass $m_{\beta\beta}$ in $0\nu\beta\beta$-decay, and the kinematical mass m_β in beta decay at the minimum values of χ^2 for all viable models $\{C_m^{(k_1,k_2,k_3)}, W_j\}$ without gCP symmetry. The best fit values of the charged lepton masses represent their global best fit values. The best fit values of the mass sum $\sum_{i=1}^3 m_i$ and $\Delta m^2_{21}/\Delta m^2_{31}$ can be easily obtained from the three neutrino masses. Therefore, these are not shown in the following tables.

Models	Best fit results for 148 viable models $\{C_m^{(k_1,k_2,k_3)}, W_j\}$ without gCP								
$\{C_m^{(k_1,k_2,k_3)}, W_j\}$	$\Re\langle\tau\rangle$	$\Im\langle\tau\rangle$	β/α	γ/α	$\lvert g_2/g_1\rvert$	$\arg(g_2/g_1)/\pi$	αv/MeV	$(g_1 v^2/\Lambda)$/meV	$\chi^2_{\rm min}$
$\{C_1^{(-4,-2,0)}, W_1\}$	−0.1647	1.092	35.10	836.8	0.4475	0.2843	5.803	910.7	8.396
$\{C_1^{(-4,-2,4)}, W_1\}$	0.1311	1.131	0.004638	2.523	0.6208	1.735	593.8	637.4	3.255
$\{C_1^{(-4,0,4)}, W_1\}$	−0.1312	1.131	0.01677	2.523	0.6213	0.2651	593.8	637.5	0.1485
$\{C_1^{(-4,2,4)}, W_1\}$	0.1311	1.131	0.002697	2.523	0.6207	1.735	593.9	637.5	3.253
$\{C_1^{(-2,2,4)}, W_1\}$	0.09140	1.180	0.005753	7.985	1.191	0.1587	197.9	330.1	9.043
$\{C_2^{(-4,-2,2)}, W_3\}$	−0.1123	1.107	1532.0	100.4	3.200	0.9246	1.925	180.5	5.904
$\{C_2^{(-2,0,2)}, W_1\}$	−0.4459	1.025	24.65	0.002108	2.241	1.973	238.5	382.9	9.741
$\{C_2^{(-2,0,4)}, W_1\}$	−0.4459	1.025	24.65	0.006334	2.241	1.973	238.5	382.9	9.769
$\{C_2^{(-2,2,4)}, W_3\}$	−0.1123	1.107	0.06556	0.0001801	2.910	1.155	2949.0	198.4	5.902
$\{C_3^{(-4,-2,2)}, W_1\}$	−0.008584	1.082	248.8	883.8	1.296	0.8024	1.706	513.1	0.2115
$\{C_3^{(-2,-2,4)}, W_1\}$	−0.008664	1.082	3.552	0.0009956	1.305	0.8055	424.3	509.5	0.2114
$\{C_4^{(-4,-2,-2)}, W_3\}$	0.3203	0.9637	65.81	1065.0	3.868	2.000	3.530	186.9	12.21
$\{C_4^{(-4,-2,0)}, W_1\}$	0.4104	0.9907	0.007602	14.52	1.182	1.943	423.4	746.7	3.888
$\{C_4^{(-4,0,0)}, W_1\}$	0.4104	0.9906	0.006390	14.52	1.182	1.943	423.4	746.8	3.886
$\{C_4^{(-4,2,0)}, W_1\}$	0.3623	1.072	210.2	43.32	1.704	0.06455	7.318	394.9	0.1512
$\{C_4^{(-4,4,-4)}, W_1\}$	−0.1311	1.131	2.523	0.004535	0.6214	0.2651	593.9	637.4	0.1479
$\{C_4^{(-4,4,-2)}, W_1\}$	−0.1556	1.146	2.972	0.002283	1.314	1.924	510.3	345.0	23.55
$\{C_4^{(-4,4,0)}, W_1\}$	0.4127	1.016	46.96	1651.0	2.175	0.04709	3.558	406.5	0.3034
$\{C_4^{(-4,4,4)}, W_1\}$	−0.1142	1.107	0.03911	0.0005010	0.6275	0.2834	5079.0	712.1	0.8468
$\{C_4^{(-2,0,-2)}, W_1\}$	−0.1647	1.092	23.84	0.004720	0.4477	0.2843	203.7	910.4	8.399
$\{C_4^{(-2,0,-2)}, W_3\}$	0.3203	0.9639	0.007490	16.17	3.719	0.08817	232.3	194.3	12.20
$\{C_4^{(-2,2,0)}, W_1\}$	0.3622	1.072	595.4	122.7	1.704	0.06457	2.584	395.0	0.1507
$\{C_4^{(-2,4,-2)}, W_1\}$	0.09126	1.180	7.986	0.004531	1.191	0.1588	197.9	330.1	9.050

Continued on next page

Table 4-continued from previous page

Models	Best fit results for 148 viable models $\{C_m^{(k_1,k_2,k_3)}, W_j\}$ without gCP								
$\{C_m^{(k_1,k_2,k_3)}, W_j\}$	$\Re\langle\tau\rangle$	$\Im\langle\tau\rangle$	β/α	γ/α	$\lvert g_2/g_1\rvert$	$\arg(g_2/g_1)/\pi$	αv/MeV	(g_1v^2/Λ)/meV	$\chi^2_{\min}$
$\{C_4^{(-2,4,0)}, W_1\}$	−0.2507	0.9983	240.4	216.6	1.276	1.772	4.976	670.3	0.08952
$\{C_4^{(-2,4,2)}, W_1\}$	0.09118	1.180	7.986	0.002364	1.190	0.1588	197.9	330.1	9.054
$\{C_4^{(0,2,0)}, W_1\}$	0.3623	1.072	491.0	101.2	1.704	0.06455	3.133	394.9	0.1514
$\{C_4^{(0,4,0)}, W_1\}$	−0.2507	0.9983	323.8	291.8	1.276	1.772	3.694	670.3	0.08944
$\{C_4^{(2,4,0)}, W_1\}$	−0.2507	0.9983	1090.0	982.3	1.276	1.772	1.097	670.2	0.08900
$\{C_5^{(-4,-2,-4)}, W_1\}$	−0.3445	0.9915	35.40	651.9	1.211	0.1022	10.54	703.5	5.073
$\{C_5^{(-4,-2,-2)}, W_1\}$	0.3844	1.062	0.04048	0.0001865	0.8533	1.935	5575.0	674.5	11.83
$\{C_5^{(-4,-2,2)}, W_1\}$	0.4337	1.003	193.9	451.2	0.3951	1.885	3.213	1542.0	7.968
$\{C_5^{(-4,0,-2)}, W_1\}$	−0.4649	1.022	2433.0	129.1	0.6554	0.06869	2.434	1016.0	0.1800
$\{C_5^{(-4,0,4)}, W_1\}$	0.4518	1.022	2494.0	67.72	0.5889	1.913	2.360	1089.0	0.1295
$\{C_5^{(-4,2,2)}, W_3\}$	0.3158	0.9870	19.64	317.8	2.547	1.741	4.514	269.8	6.368
$\{C_5^{(-4,4,-4)}, W_1\}$	0.1311	1.131	2.523	0.005305	0.6207	1.735	593.8	637.5	3.256
$\{C_5^{(-2,0,-4)}, W_1\}$	−0.3443	0.9914	0.005911	18.42	1.212	0.1022	373.1	703.2	5.047
$\{C_5^{(-2,0,-2)}, W_1\}$	−0.4649	1.022	1705.0	90.47	0.6554	0.06869	3.473	1016.0	0.1805
$\{C_5^{(-2,0,0)}, W_1\}$	−0.1647	1.092	23.84	0.02361	0.4484	0.2841	203.7	909.3	8.410
$\{C_5^{(-2,0,4)}, W_1\}$	0.4518	1.022	1245.0	33.81	0.5889	1.913	4.726	1089.0	0.1290
$\{C_5^{(-2,2,-4)}, W_1\}$	−0.3443	0.9915	0.005129	18.42	1.212	0.1022	373.0	703.2	5.075
$\{C_5^{(-2,2,2)}, W_1\}$	−0.006388	1.064	9.867	145.9	0.9613	0.7073	10.26	716.3	1.005
$\{C_5^{(-2,4,-4)}, W_1\}$	−0.3443	0.9914	0.003681	18.42	1.212	0.1021	373.1	703.1	5.043
$\{C_5^{(-2,4,0)}, W_1\}$	0.09103	1.180	7.988	0.01439	1.190	0.1589	197.8	330.1	9.064
$\{C_5^{(0,2,2)}, W_1\}$	−0.004932	1.049	70.75	1044.0	0.8506	0.3137	1.416	797.0	6.627
$\{C_5^{(0,4,-2)}, W_1\}$	0.4647	1.023	0.0001353	0.05294	0.6523	1.931	5916.0	1016.0	1.259
$\{C_5^{(2,4,-4)}, W_1\}$	−0.2531	1.031	14.41	0.06271	1.572	1.907	89.43	492.5	17.74
$\{C_5^{(2,4,0)}, W_1\}$	0.2460	1.004	1082.0	422.2	1.447	0.1607	1.134	582.4	11.56
$\{C_6^{(-4,0,-4)}, W_1\}$	0.4103	0.9907	2647.0	182.3	1.182	1.943	2.323	746.8	3.887
$\{C_6^{(-4,0,-2)}, W_1\}$	0.3600	0.9758	2380.0	122.7	1.830	0.1372	2.633	545.1	10.31
$\{C_6^{(-4,0,2)}, W_1\}$	0.3622	1.072	133.1	645.9	1.704	0.06456	2.382	394.8	0.1511
$\{C_6^{(-4,0,4)}, W_1\}$	−0.2507	0.9983	341.2	378.6	1.276	1.772	3.159	670.3	0.08941
$\{C_6^{(-2,0,-4)}, W_1\}$	0.4104	0.9906	2280.0	156.9	1.182	1.943	2.698	746.7	3.891
$\{C_6^{(-2,0,-2)}, W_1\}$	−0.4458	1.025	24.65	0.01579	2.241	1.973	238.5	382.9	9.737
$\{C_6^{(-2,0,0)}, W_1\}$	0.4459	1.026	24.60	0.009334	2.233	0.02595	238.5	382.9	13.77
$\{C_6^{(-2,0,2)}, W_1\}$	0.3622	1.072	98.90	479.9	1.704	0.06457	3.206	394.8	0.1511
$\{C_6^{(-2,0,4)}, W_1\}$	−0.2507	0.9983	740.0	821.3	1.276	1.772	1.456	670.3	0.08918
$\{C_6^{(0,4,-2)}, W_1\}$	0.3581	0.9764	0.0001221	0.05286	1.821	0.1384	6064.0	545.2	10.47
$\{C_6^{(0,4,2)}, W_1\}$	0.3621	1.072	0.01010	4.853	1.704	0.06459	317.0	395.0	0.1501
$\{C_7^{(-4,4,-4)}, W_1\}$	0.2772	0.9663	37.49	3152.0	1.506	0.09314	2.333	621.9	13.64
$\{C_7^{(-2,0,-4)}, W_1\}$	−0.4459	1.025	24.65	0.01454	2.241	1.973	238.5	382.9	9.740
$\{C_7^{(-2,0,-2)}, W_1\}$	−0.4459	1.025	24.65	0.004217	2.241	1.973	238.5	382.9	9.742
$\{C_7^{(-2,0,0)}, W_1\}$	0.3639	0.9622	3030.0	246.3	1.165	1.844	2.036	822.6	0.1510
$\{C_7^{(-2,2,0)}, W_3\}$	−0.1115	1.109	0.06592	0.0005472	3.104	1.107	2943.0	186.1	5.886

Continued on next page

Table 4-continued from previous page

Models	Best fit results for 148 viable models $\{C_m^{(k_1,k_2,k_3)}, W_j\}$ without gCP								
$\{C_m^{(k_1,k_2,k_3)}, W_j\}$	$\Re\langle\tau\rangle$	$\Im\langle\tau\rangle$	β/α	γ/α	$\lvert g_2/g_1\rvert$	$\arg(g_2/g_1)/\pi$	αv/MeV	(g_1v^2/Λ)/meV	$\chi^2_{\min}$
$\{C_7^{(-2,2,2)}, W_1\}$	0.1050	1.043	32.25	482.1	0.9410	0.3121	3.063	773.8	0.2972
$\{C_7^{(-2,2,2)}, W_3\}$	0.2289	1.002	0.003423	6.993	2.947	1.792	205.8	215.3	5.992
$\{C_7^{(-2,2,4)}, W_3\}$	−0.1126	1.107	0.06538	0.0001784	2.855	0.8339	2952.0	202.3	5.922
$\{C_7^{(-2,4,2)}, W_3\}$	−0.3541	0.9644	0.003544	6.325	3.527	1.834	223.2	217.7	8.903
$\{C_7^{(0,2,2)}, W_1\}$	0.1050	1.043	64.82	968.9	0.9409	0.3122	1.524	773.9	0.2976
$\{C_7^{(0,4,-4)}, W_1\}$	0.2772	0.9663	16.33	1373.0	1.506	0.09317	5.356	622.0	13.66
$\{C_8^{(-4,-2,0)}, W_1\}$	−0.4649	1.022	106.4	2005.0	0.6554	0.06869	2.954	1016.0	0.1803
$\{C_8^{(-4,2,-2)}, W_1\}$	−0.008550	1.036	784.3	181.2	1.179	0.7699	1.860	614.8	1.805
$\{C_8^{(-4,2,2)}, W_1\}$	0.006295	1.064	848.2	57.38	0.9478	1.296	1.765	726.1	3.411
$\{C_8^{(-4,2,2)}, W_3\}$	−0.3158	0.9870	283.7	17.53	2.667	0.2445	5.056	257.6	3.311
$\{C_8^{(-4,4,0)}, W_1\}$	0.4518	1.022	47.83	1761.0	0.5889	1.913	3.341	1089.0	0.1293
$\{C_8^{(-2,0,0)}, W_1\}$	−0.4649	1.022	0.006326	18.85	0.6554	0.06869	314.2	1016.0	0.1801
$\{C_8^{(-2,0,4)}, W_1\}$	0.2460	1.004	448.7	1150.0	1.447	0.1608	1.068	582.4	11.55
$\{C_8^{(-2,2,-2)}, W_1\}$	−0.006594	1.036	85.14	19.65	0.9052	0.6956	17.13	800.1	1.473
$\{C_8^{(-2,2,0)}, W_1\}$	−0.4649	1.022	0.003024	18.85	0.6554	0.06869	314.2	1016.0	0.1804
$\{C_8^{(-2,2,2)}, W_1\}$	−0.006292	1.064	47.73	3.220	0.9475	0.7038	31.36	726.5	0.9992
$\{C_8^{(-2,4,0)}, W_1\}$	0.4518	1.022	15.14	557.9	0.5885	1.913	10.55	1089.0	0.1296
$\{C_8^{(0,2,2)}, W_1\}$	−0.006399	1.064	1038.0	70.19	0.9631	0.7077	1.443	714.8	1.005
$\{C_8^{(0,4,0)}, W_1\}$	0.4518	1.022	78.53	2892.0	0.5884	1.913	2.035	1090.0	0.1289
$\{C_8^{(2,4,-2)}, W_1\}$	0.2634	1.067	0.0003294	0.2366	1.089	1.852	1515.0	544.6	15.29
$\{C_8^{(2,4,0)}, W_1\}$	0.4518	1.022	137.1	5050.0	0.5884	1.913	1.165	1090.0	0.1286
$\{C_9^{(-4,0,0)}, W_1\}$	0.3639	0.9622	78.02	959.8	1.165	1.844	6.428	822.6	0.1505
$\{C_9^{(-4,2,-2)}, W_3\}$	0.2289	1.002	500.8	71.62	3.304	0.1502	2.874	192.0	5.994
$\{C_9^{(-4,2,2)}, W_1\}$	0.1048	1.044	753.4	50.41	0.9404	0.3122	1.960	774.2	0.2971
$\{C_9^{(-4,2,4)}, W_1\}$	0.2771	0.9662	0.0001420	0.01189	1.505	0.09315	7355.0	622.2	13.68
$\{C_9^{(-4,4,4)}, W_1\}$	−0.2774	0.9663	0.00005048	0.01189	1.510	1.909	7353.0	620.2	15.14
$\{C_9^{(-2,2,-4)}, W_1\}$	−0.008753	1.082	3.552	0.003759	1.315	0.8091	424.3	505.6	0.2121
$\{C_9^{(-2,2,-2)}, W_1\}$	0.07443	1.042	310.6	40.22	0.9243	0.3142	4.742	786.4	5.592
$\{C_9^{(-2,2,-2)} W_3\}$	0.2289	1.002	832.7	119.1	3.615	0.07222	1.728	175.5	5.993
$\{C_9^{(-2,2,2)}, W_1\}$	0.1049	1.044	223.3	14.93	0.9407	0.3122	6.613	773.9	0.2984
$\{C_9^{(0,2,-2)}, W_3\}$	0.2289	1.002	820.6	117.4	3.709	0.002393	1.754	171.0	5.994
$\{C_9^{(0,2,0)}, W_1\}$	−0.3640	0.9622	0.001613	12.31	1.165	0.1558	501.3	823.0	3.257
$\{C_9^{(0,2,2)}, W_1\}$	0.1050	1.043	1015.0	67.92	0.9409	0.3122	1.454	773.9	0.2977
$\{C_9^{(2,4,-2)}, W_1\}$	−0.07406	1.042	0.004392	37.25	0.9235	1.686	86.84	786.8	41.48
$\{C_9^{(2,4,-2)}, W_3\}$	0.06938	1.127	0.004924	31.05	2.592	0.7960	92.43	221.9	7.010
$\{C_9^{(2,4,2)}, W_1\}$	0.1054	1.043	0.0002727	0.06689	0.9420	0.3120	1476.0	773.2	0.2988
$\{C_{10}^{(-4,-2,2)}, W_1\}$	0.07447	1.042	105.2	812.6	0.9237	0.3143	1.813	786.7	5.598
$\{C_{10}^{(-4,0,4)}, W_1\}$	0.3629	0.9812	13.21	0.0008582	1.739	0.07663	458.9	559.5	21.04
$\{C_{10}^{(-4,2,2)}, W_1\}$	0.1031	1.044	56.35	841.9	0.9361	0.3130	1.754	777.2	0.2947
$\{C_{10}^{(-4,4,-4)}, W_1\}$	0.2771	0.9663	7.863	660.8	1.505	0.09351	11.13	622.0	13.83

Continued on next page

Table 4-continued from previous page

Models	Best fit results for 148 viable models $\{C_m^{(k_1,k_2,k_3)}, W_j\}$ without gCP								
$\{C_m^{(k_1,k_2,k_3)}, W_j\}$	$\Re\langle\tau\rangle$	$\Im\langle\tau\rangle$	β/α	γ/α	$\lvert g_2/g_1\rvert$	$\arg(g_2/g_1)/\pi$	αv/MeV	(g_1v^2/Λ)/meV	$\chi^2_{\rm min}$
$\{C_{10}^{(-2,-4,-4)}, W_1\}$	−0.3443	0.9914	0.005477	18.42	1.212	0.1022	373.2	703.2	5.050
$\{C_{10}^{(-2,-2,-4)}, W_1\}$	0.3427	0.9919	0.005623	18.53	1.230	1.902	370.5	693.3	8.413
$\{C_{10}^{(-2,-2,-4)}, W_3\}$	0.3203	0.9636	16.18	0.03275	3.007	0.2166	232.3	240.5	12.19
$\{C_{10}^{(-2,-2,-2)}, W_3\}$	0.3203	0.9637	16.18	0.005280	3.524	0.1352	232.3	205.2	12.21
$\{C_{10}^{(-2,-2,2)}, W_1\}$	0.07438	1.042	33.44	258.3	0.9240	0.3142	5.703	786.6	5.586
$\{C_{10}^{(-2,-2,2)}, W_3\}$	0.2289	1.002	34.05	238.1	2.958	0.2062	6.044	214.4	5.991
$\{C_{10}^{(-2,0,-4)}, W_1\}$	−0.3443	0.9915	0.01121	18.42	1.212	0.1022	373.1	703.1	5.051
$\{C_{10}^{(-2,0,-2)}, W_1\}$	0.3580	0.9764	18.92	0.003735	1.821	0.1384	320.4	545.1	10.57
$\{C_{10}^{(-2,0,0)}, W_1\}$	0.3639	0.9622	1574.0	128.0	1.165	1.844	3.919	822.6	0.1504
$\{C_{10}^{(-2,0,2)}, W_1\}$	0.006629	1.036	0.004140	4.329	0.9090	1.303	336.9	796.4	3.958
$\{C_{10}^{(-2,2,-4)}, W_1\}$	−0.3444	0.9914	0.001096	18.41	1.212	0.1022	373.3	703.4	5.054
$\{C_{10}^{(-2,2,2)}, W_1\}$	0.1043	1.044	21.52	321.6	0.9393	0.3125	4.591	774.9	0.2959
$\{C_{10}^{(-2,4,-4)}, W_1\}$	0.2767	0.9667	2.826	237.9	1.503	0.09493	30.88	621.9	14.25
$\{C_{10}^{(-2,4,2)}, W_1\}$	0.4336	1.003	0.0007264	2.326	0.3953	1.885	623.2	1542.0	7.972
$\{C_{10}^{(0,-2,2)}, W_1\}$	0.07425	1.042	136.0	1050.0	0.9234	0.3144	1.402	786.8	5.589
$\{C_{10}^{(0,-2,2)}, W_3\}$	0.2289	1.002	134.1	937.8	3.710	1.998	1.535	171.0	5.993
$\{C_{10}^{(0,2,2)}, W_1\}$	0.1045	1.044	67.68	1012.0	0.9397	0.3124	1.459	774.8	0.2965
$\{C_{10}^{(0,4,-4)}, W_1\}$	0.2758	0.9668	38.18	3191.0	1.500	0.09608	2.302	622.5	13.57
$\{C_{10}^{(2,-4,2)}, W_1\}$	−0.006413	1.064	0.01650	14.78	0.9652	0.7083	101.2	713.3	1.005
$\{C_{10}^{(2,-4,2)}, W_3\}$	−0.3158	0.9870	0.02204	16.18	3.690	0.03111	88.65	186.2	3.313
$\{C_{10}^{(2,-2,-2)}, W_1\}$	−0.06747	1.049	20.80	0.01857	0.9093	1.686	153.5	776.0	36.70
$\{C_{10}^{(2,-2,0)}, W_1\}$	−0.06757	1.049	20.80	0.009149	0.9084	1.686	153.5	776.3	36.60
$\{C_{10}^{(2,-2,2)}, W_1\}$	0.07440	1.042	70.53	544.8	0.9245	0.3141	2.704	786.5	5.590
$\{C_{10}^{(2,-2,2)}, W_3\}$	−0.3159	0.9870	0.05133	16.19	3.701	0.02016	88.63	185.7	3.315
$\{C_{10}^{(2,-2,4)}, W_1\}$	−0.06757	1.049	20.80	0.002536	0.9064	1.685	153.4	777.0	36.66
$\{C_{10}^{(2,0,-4)}, W_1\}$	0.3622	1.072	0.2061	0.001565	1.704	0.06460	1538.0	394.8	0.1509
$\{C_{10}^{(2,0,-2)}, W_1\}$	0.3585	0.9683	72.88	0.01259	1.451	1.936	84.03	670.4	23.44
$\{C_{10}^{(2,0,0)}, W_1\}$	0.3639	0.9622	4643.0	377.4	1.165	1.844	1.329	822.6	0.1513
$\{C_{10}^{(2,0,2)}, W_1\}$	0.005025	1.049	0.01382	14.75	0.8496	1.686	100.2	797.4	10.13
$\{C_{10}^{(2,0,2)}, W_3\}$	−0.3158	0.9870	0.02714	16.18	2.499	1.735	88.65	274.9	3.311
$\{C_{10}^{(2,0,4)}, W_1\}$	0.3623	1.072	0.2061	0.0002852	1.704	0.06456	1538.0	394.9	0.1512
$\{C_{10}^{(2,2,2)}, W_1\}$	0.1049	1.043	90.51	1353.0	0.9409	0.3122	1.091	773.9	0.2973
$\{C_{10}^{(2,2,2)}, W_3\}$	−0.3158	0.9870	0.005264	16.18	2.952	1.793	88.65	232.7	3.313
$\{C_{10}^{(2,4,-4)}, W_1\}$	0.2756	0.9669	41.14	3435.0	1.494	0.09976	2.138	624.2	13.40
$\{C_{10}^{(2,4,2)}, W_3\}$	−0.3158	0.9870	0.01080	16.18	2.494	1.735	88.64	275.6	3.309
$\{C_{10}^{(4,-2,2)}, W_1\}$	0.07443	1.042	492.5	3803.0	0.9239	0.3142	0.3873	786.7	5.591
$\{C_{10}^{(4,0,-4)}, W_1\}$	−0.3715	0.9997	31.64	0.02805	2.035	1.898	186.5	460.9	0.5692
$\{C_{10}^{(4,0,-2)}, W_1\}$	−0.3715	0.9997	31.64	0.005841	2.035	1.898	186.5	461.0	0.5691
$\{C_{10}^{(4,0,0)}, W_1\}$	0.3639	0.9622	2677.0	217.6	1.165	1.844	2.305	822.6	0.1506
$\{C_{10}^{(4,0,2)}, W_1\}$	0.4129	1.016	35.18	0.005630	2.176	0.04688	167.0	406.4	0.3006

Continued on next page

Table 4-continued from previous page

Models	Best fit results for 148 viable models $\{C_m^{(k_1,k_2,k_3)}, W_j\}$ without gCP										
$\{C_m^{(k_1,k_2,k_3)}, W_j\}$	$\Re\langle\tau\rangle$	$\Im\langle\tau\rangle$	β/α	γ/α	$\lvert g_2/g_1\rvert$	$\arg(g_2/g_1)/\pi$	αv/MeV	$(g_1 v^2/\Lambda)$/meV	$\chi^2_{\min}$		
$\{C_{10}^{(4,0,4)}, W_1\}$	0.4128	1.016	35.17	0.002216	2.176	0.04702	167.1	406.5	0.3015		
$\{C_{10}^{(4,2,2)}, W_1\}$	0.1023	1.044	237.7	3551.0	0.9339	0.3134	0.4158	778.7	0.2950		
$\{C_{10}^{(4,4,-4)}, W_1\}$	0.2773	0.9663	65.83	5535.0	1.506	0.09308	1.329	621.9	13.61		
$\{C_{10}^{(4,4,0)}, W_1\}$	0.2515	0.9679	0.07247	0.006658	1.304	1.839	1144.0	685.0	32.39		
$\{C_m^{(k_1,k_2,k_3)}, W_j\}$	$\sin^2\theta_{13}$	$\sin^2\theta_{12}$	$\sin^2\theta_{23}$	$\delta_{\rm CP}/\pi$	α_{21}/π	α_{31}/π	m_1/meV	m_2/meV	m_3/meV	$m_{\beta\beta}$/meV	m_β/meV
$\{C_1^{(-4,-2,0)}, W_1\}$	0.02237	0.3103	0.4677	1.591	0.1900	0.06329	29.33	30.56	57.71	26.85	30.62
$\{C_1^{(-4,-2,4)}, W_1\}$	0.02216	0.3080	0.4698	0.7670	1.897	1.757	22.44	24.03	54.58	23.02	24.10
$\{C_1^{(-4,0,4)}, W_1\}$	0.02215	0.3080	0.4699	1.233	0.1038	0.2430	22.43	24.02	54.60	23.01	24.09
$\{C_1^{(-4,2,4)}, W_1\}$	0.02216	0.3080	0.4698	0.7672	1.897	1.758	22.44	24.03	54.58	23.02	24.10
$\{C_1^{(-2,2,4)}, W_1\}$	0.02235	0.3089	0.4656	1.607	0.004682	1.554	12.62	15.27	51.27	13.73	15.39
$\{C_2^{(-4,-2,2)}, W_3\}$	0.02216	0.3108	0.4496	1.475	1.676	1.434	22.02	23.64	54.44	19.30	23.71
$\{C_2^{(-2,0,2)}, W_1\}$	0.02212	0.3392	0.4855	1.395	0.9473	1.768	21.78	23.41	54.51	5.386	23.54
$\{C_2^{(-2,0,4)}, W_1\}$	0.02212	0.3392	0.4856	1.395	0.9474	1.768	21.78	23.41	54.51	5.384	23.54
$\{C_2^{(-2,2,4)}, W_3\}$	0.02216	0.3108	0.4496	1.474	1.307	1.321	23.52	25.04	55.07	13.04	25.11
$\{C_3^{(-4,-2,2)}, W_1\}$	0.02215	0.3080	0.4787	1.175	1.664	1.506	23.61	25.13	55.11	19.96	25.19
$\{C_3^{(-2,-2,4)}, W_1\}$	0.02215	0.3080	0.4787	1.178	1.663	1.510	23.47	24.99	55.05	19.81	25.06
$\{C_4^{(-4,-2,-4)}, W_1\}$	0.02254	0.3103	0.4644	1.662	1.195	1.619	12.32	15.02	51.29	5.534	15.17
$\{C_4^{(4,-2,-2)}, W_3\}$	0.02200	0.3068	0.5357	1.085	0.9383	1.965	22.08	23.69	54.47	8.970	23.75
$\{C_4^{(-4,-2,0)}, W_1\}$	0.02211	0.3103	0.4714	1.461	0.8938	1.590	19.60	21.40	53.53	7.211	21.48
$\{C_4^{(-4,0,0)}, W_1\}$	0.02211	0.3103	0.4714	1.461	0.8937	1.590	19.60	21.40	53.53	7.212	21.48
$\{C_4^{(-4,2,0)}, W_1\}$	0.02216	0.3083	0.4698	1.090	1.153	0.1964	17.39	19.40	52.75	8.182	19.48
$\{C_4^{(-4,4,-4)}, W_1\}$	0.02215	0.3080	0.4699	1.233	0.1037	0.2429	22.43	24.02	54.60	23.00	24.09
$\{C_4^{(-4,4,-2)}, W_1\}$	0.02221	0.3079	0.4720	1.878	0.4132	0.9088	11.33	14.22	51.22	8.598	14.35
$\{C_4^{(-4,4,0)}, W_1\}$	0.02211	0.3088	0.4718	1.056	1.378	0.5227	22.11	23.72	54.51	13.76	23.79
$\{C_4^{(-4,4,4)}, W_1\}$	0.02215	0.3080	0.4703	0.9683	0.1040	1.682	24.90	26.34	55.69	25.28	26.40
$\{C_4^{(-2,0,-2)}, W_1\}$	0.02237	0.3103	0.4677	1.591	0.1899	0.06328	29.32	30.55	57.70	26.84	30.61
$\{C_4^{(-2,0,-2)}, W_3\}$	0.02203	0.3071	0.5358	1.086	1.083	0.07103	22.70	24.27	54.72	9.750	24.33
$\{C_4^{(-2,2,0)}, W_1\}$	0.02216	0.3083	0.4698	1.090	1.153	0.1967	17.39	19.40	52.75	8.186	19.48
$\{C_4^{(-2,4,-2)}, W_1\}$	0.02235	0.3089	0.4656	1.607	0.004791	1.554	12.62	15.27	51.27	13.73	15.39
$\{C_4^{(-2,4,0)}, W_1\}$	0.02215	0.3080	0.4703	1.110	0.4265	1.283	22.20	23.81	54.51	16.88	23.88
$\{C_4^{(-2,4,2)}, W_1\}$	0.02235	0.3089	0.4656	1.607	0.004840	1.554	12.62	15.27	51.27	13.73	15.39
$\{C_4^{(0,2,0)}, W_1\}$	0.02216	0.3083	0.4698	1.090	1.153	0.1964	17.39	19.40	52.75	8.182	19.48
$\{C_4^{(0,4,0)}, W_1\}$	0.02215	0.3079	0.4703	1.110	0.4266	1.283	22.20	23.81	54.51	16.88	23.88
$\{C_4^{(2,4,0)}, W_1\}$	0.02215	0.3079	0.4703	1.110	0.4267	1.284	22.20	23.81	54.51	16.88	23.88
$\{C_5^{(-4,-2,-2)}, W_1\}$	0.02254	0.3103	0.4642	1.661	1.194	1.619	12.32	15.02	51.29	5.526	15.17
$\{C_5^{(-4,-2,2)}, W_1\}$	0.02216	0.3053	0.4899	1.554	1.379	1.291	16.93	18.99	52.51	11.36	19.07
$\{C_5^{(-4,0,-2)}, W_1\}$	0.02215	0.3080	0.4711	1.082	0.6277	0.4378	14.32	16.70	51.82	10.10	16.80
$\{C_5^{(-4,0,4)}, W_1\}$	0.02215	0.3079	0.4694	1.096	1.557	1.668	14.28	16.67	51.80	12.11	16.76
$\{C_5^{(-4,2,2)}, W_3\}$	0.02209	0.3081	0.5039	0.7716	0.6327	1.701	28.40	29.67	57.32	18.88	29.72
$\{C_5^{(-4,4,-4)}, W_1\}$	0.02216	0.3080	0.4698	0.7670	1.897	1.757	22.44	24.03	54.59	23.02	24.10

Continued on next page

Table 4-continued from previous page

$\{C_m^{(k_1,k_2,k_3)}, W_j\}$	$\sin^2\theta_{13}$	$\sin^2\theta_{12}$	$\sin^2\theta_{23}$	δ_{CP}/π	α_{21}/π	α_{31}/π	m_1/meV	m_2/meV	m_3/meV	$m_{\beta\beta}$/meV	m_β/meV
$\{C_5^{(-2,0,-4)}, W_1\}$	0.02251	0.3321	0.4792	1.269	0.8271	0.1349	18.79	20.66	53.32	7.271	20.81
$\{C_5^{(-2,0,-2)}, W_1\}$	0.02215	0.3080	0.4711	1.082	0.6276	0.4377	14.32	16.70	51.82	10.10	16.80
$\{C_5^{(-2,0,0)}, W_1\}$	0.02237	0.3103	0.4677	1.591	0.1899	0.06322	29.27	30.51	57.68	26.80	30.57
$\{C_5^{(-2,0,4)}, W_1\}$	0.02215	0.3079	0.4694	1.097	1.557	1.668	14.28	16.67	51.80	12.11	16.76
$\{C_5^{(-2,2,-4)}, W_1\}$	0.02251	0.3321	0.4793	1.269	0.8271	0.1349	18.79	20.66	53.32	7.267	20.81
$\{C_5^{(-2,2,2)}, W_1\}$	0.02216	0.3080	0.4890	1.179	1.847	1.479	29.55	30.78	57.90	27.44	30.83
$\{C_5^{(-2,4,-4)}, W_1\}$	0.02251	0.3320	0.4791	1.268	0.8272	0.1349	18.79	20.67	53.33	7.272	20.82
$\{C_5^{(-2,4,0)}, W_1\}$	0.02235	0.3089	0.4656	1.607	0.004950	1.555	12.62	15.27	51.27	13.73	15.39
$\{C_5^{(0,2,2)}, W_1\}$	0.02216	0.3066	0.5172	1.273	1.868	0.3666	29.92	31.13	58.14	30.25	31.18
$\{C_5^{(0,4,-2)}, W_1\}$	0.02215	0.3079	0.4688	0.9229	1.379	1.568	14.26	16.65	51.78	10.17	16.75
$\{C_5^{(2,4,-4)}, W_1\}$	0.02291	0.3083	0.4368	1.672	0.6685	1.470	19.06	20.91	53.38	12.34	21.04
$\{C_5^{(2,4,0)}, W_1\}$	0.02210	0.3083	0.4731	1.668	1.772	0.7992	20.72	22.43	53.87	19.80	22.50
$\{C_6^{(-4,0,-4)}, W_1\}$	0.02211	0.3102	0.4716	1.461	0.8934	1.590	19.59	21.39	53.53	7.215	21.47
$\{C_6^{(-4,0,-2)}, W_1\}$	0.02334	0.3105	0.4381	1.364	1.681	0.7203	23.38	24.91	54.62	22.03	25.02
$\{C_6^{(-4,0,2)}, W_1\}$	0.02216	0.3083	0.4697	1.090	1.153	0.1966	17.39	19.39	52.75	8.183	19.48
$\{C_6^{(-4,0,4)}, W_1\}$	0.02215	0.3079	0.4703	1.110	0.4266	1.283	22.20	23.81	54.51	16.88	23.88
$\{C_6^{(-2,0,-4)}, W_1\}$	0.02211	0.3103	0.4714	1.461	0.8937	1.590	19.60	21.40	53.53	7.212	21.48
$\{C_6^{(-2,0,-2)}, W_1\}$	0.02212	0.3391	0.4855	1.395	0.9473	1.768	21.78	23.41	54.51	5.386	23.54
$\{C_6^{(-2,0,0)}, W_1\}$	0.02212	0.3385	0.4891	0.6098	1.055	0.2351	21.71	23.35	54.50	5.410	23.47
$\{C_6^{(-2,0,2)}, W_1\}$	0.02216	0.3083	0.4697	1.090	1.153	0.1967	17.39	19.40	52.75	8.184	19.48
$\{C_6^{(-2,0,4)}, W_1\}$	0.02215	0.3079	0.4703	1.110	0.4266	1.284	22.20	23.81	54.51	16.88	23.88
$\{C_6^{(0,4,-2)}, W_1\}$	0.02351	0.3112	0.4439	1.363	1.682	0.7210	23.30	24.84	54.53	21.98	24.95
$\{C_6^{(0,4,2)}, W_1\}$	0.02216	0.3083	0.4698	1.090	1.153	0.1969	17.39	19.40	52.75	8.189	19.49
$\{C_7^{(-4,4,-4)}, W_1\}$	0.02212	0.3392	0.4855	1.395	0.9474	1.768	21.78	23.41	54.51	5.386	23.54
$\{C_7^{(-2,0,-4)}, W_1\}$	0.02215	0.3080	0.4746	1.066	1.942	0.4009	29.32	30.56	57.78	29.76	30.61
$\{C_7^{(-2,0,-2)}, W_1\}$	0.02372	0.3086	0.5173	1.109	1.191	0.2243	20.42	22.16	53.86	10.25	22.32
$\{C_7^{(-2,0,0)}, W_1\}$	0.02215	0.3083	0.4697	1.234	0.6553	1.395	20.77	22.48	53.96	11.55	22.55
$\{C_7^{(-2,2,0)}, W_3\}$	0.02211	0.3118	0.4491	1.469	1.382	1.340	22.56	24.15	54.67	14.10	24.22
$\{C_7^{(-2,2,2)}, W_1\}$	0.02215	0.3080	0.4746	1.067	1.942	0.4009	29.32	30.55	57.78	29.75	30.61
$\{C_7^{(-2,2,2)}, W_3\}$	0.02215	0.3081	0.4985	1.457	1.389	1.129	22.81	24.38	54.77	15.17	24.44
$\{C_7^{(-2,2,4)}, W_3\}$	0.02218	0.3102	0.4498	1.477	1.829	1.480	23.80	25.31	55.19	22.71	25.37
$\{C_7^{(-2,4,2)}, W_3\}$	0.02216	0.3080	0.4983	1.551	0.7500	1.811	26.10	27.48	56.22	13.00	27.54
$\{C_7^{(0,2,2)}, W_1\}$	0.02215	0.3080	0.4746	1.066	1.942	0.4009	29.32	30.56	57.78	29.76	30.61
$\{C_7^{(0,4,-4)}, W_1\}$	0.02372	0.3086	0.5173	1.109	1.191	0.2244	20.42	22.16	53.86	10.26	22.32
$\{C_8^{(-4,-2,0)}, W_1\}$	0.02215	0.3080	0.4711	1.082	0.6277	0.4377	14.32	16.70	51.82	10.10	16.80
$\{C_8^{(-4,2,-2)}, W_1\}$	0.02216	0.3080	0.4931	1.261	1.945	1.651	23.07	24.62	54.88	21.87	24.68
$\{C_8^{(-4,2,2)}, W_1\}$	0.02216	0.3074	0.4890	0.8248	0.1516	0.5257	29.94	31.15	58.08	27.82	31.20
$\{C_8^{(-4,2,2)}, W_3\}$	0.02210	0.3081	0.5039	1.229	1.338	0.2752	27.24	28.57	56.76	17.37	28.62
$\{C_8^{(-4,4,0)}, W_1\}$	0.02215	0.3079	0.4694	1.096	1.557	1.668	14.28	16.67	51.80	12.11	16.76
$\{C_8^{(-2,0,0)}, W_1\}$	0.02215	0.3080	0.4711	1.082	0.6277	0.4378	14.32	16.70	51.82	10.10	16.80
$\{C_8^{(-2,0,4)}, W_1\}$	0.02210	0.3083	0.4731	1.668	1.772	0.7992	20.72	22.43	53.87	19.80	22.50

Continued on next page

Table 4-continued from previous page

$\{C_m^{(k_1,k_2,k_3)}, W_j\}$	$\sin^2\theta_{13}$	$\sin^2\theta_{12}$	$\sin^2\theta_{23}$	$\delta_{\rm CP}/\pi$	α_{21}/π	α_{31}/π	m_1/meV	m_2/meV	m_3/meV	$m_{\beta\beta}$/meV	m_β/meV
$\{C_8^{(-2,2,-2)}, W_1\}$	0.02216	0.3080	0.4931	1.180	1.956	1.535	30.05	31.26	58.16	28.63	31.31
$\{C_8^{(-2,2,0)}, W_1\}$	0.02215	0.3080	0.4711	1.082	0.6277	0.4377	14.32	16.70	51.82	10.10	16.80
$\{C_8^{(-2,2,2)}, W_1\}$	0.02216	0.3080	0.4890	1.175	1.848	1.474	29.97	31.18	58.12	27.84	31.23
$\{C_8^{(-2,4,0)}, W_1\}$	0.02215	0.3080	0.4691	1.097	1.558	1.669	14.27	16.66	51.79	12.11	16.76
$\{C_8^{(0,2,2)}, W_1\}$	0.02216	0.3080	0.4890	1.180	1.846	1.480	29.50	30.73	57.87	27.38	30.78
$\{C_8^{(0,4,0)}, W_1\}$	0.02215	0.3080	0.4691	1.097	1.558	1.669	14.27	16.66	51.79	12.11	16.76
$\{C_8^{(2,4,-2)}, W_1\}$	0.02162	0.2895	0.5324	1.008	0.2344	0.03570	13.71	16.18	51.97	14.40	16.22
$\{C_8^{(2,4,0)}, W_1\}$	0.02215	0.3079	0.4691	1.097	1.558	1.669	14.27	16.66	51.79	12.11	16.76
$\{C_9^{(-4,0,0)}, W_1\}$	0.02215	0.3083	0.4697	1.234	0.6553	1.395	20.77	22.48	53.96	11.55	22.55
$\{C_9^{(-4,2,-2)}, W_3\}$	0.02215	0.3081	0.4985	1.457	0.7475	0.9243	20.62	22.34	53.89	11.49	22.42
$\{C_9^{(-4,2,2)}, W_1\}$	0.02215	0.3080	0.4747	1.067	1.943	0.4013	29.34	30.57	57.79	29.77	30.62
$\{C_9^{(-4,2,4)}, W_1\}$	0.02372	0.3084	0.5175	1.110	1.191	0.2241	20.42	22.16	53.87	10.26	22.32
$\{C_9^{(-4,4,4)}, W_1\}$	0.02374	0.3071	0.5168	0.8963	0.8139	1.781	20.42	22.15	53.85	10.21	22.31
$\{C_9^{(-2,2,-4)}, W_1\}$	0.02215	0.3080	0.4787	1.181	1.661	1.513	23.32	24.85	54.98	19.65	24.92
$\{C_9^{(-2,2,-2)}, W_1\}$	0.02218	0.3073	0.4844	1.501	0.08114	0.4909	29.93	31.14	58.10	29.30	31.19
$\{C_9^{(-2,2,-2)} W_3\}$	0.02214	0.3081	0.4985	1.457	0.8876	0.9689	19.10	20.95	53.33	8.506	21.02
$\{C_9^{(-2,2,2)}, W_1\}$	0.02216	0.3081	0.4746	1.066	1.942	0.4010	29.33	30.56	57.78	29.76	30.61
$\{C_9^{(0,2,-2)}, W_3\}$	0.02215	0.3081	0.4985	1.457	1.010	1.010	18.69	20.57	53.18	7.575	20.65
$\{C_9^{(0,2,0)}, W_1\}$	0.02215	0.3090	0.4693	0.7673	1.345	0.6068	20.78	22.49	53.97	11.55	22.56
$\{C_9^{(0,2,2)}, W_1\}$	0.02215	0.3080	0.4746	1.066	1.942	0.4009	29.32	30.56	57.78	29.75	30.61
$\{C_9^{(2,4,-2)}, W_1\}$	0.02215	0.3058	0.5848	1.499	1.919	1.507	29.94	31.15	58.10	29.32	31.20
$\{C_9^{(2,4,-2)}, W_3\}$	0.02214	0.3090	0.4367	1.413	1.336	1.092	26.66	28.01	56.48	16.03	28.07
$\{C_9^{(2,4,2)}, W_1\}$	0.02215	0.3081	0.4744	1.065	1.942	0.4002	29.29	30.53	57.77	29.72	30.58
$\{C_{10}^{(-4,-2,2)}, W_1\}$	0.02222	0.3085	0.4844	1.501	0.08112	0.4911	29.94	31.15	58.10	29.31	31.21
$\{C_{10}^{(-4,0,4)}, W_1\}$	0.02220	0.3033	0.4662	1.836	1.362	0.3164	22.62	24.20	54.68	13.04	24.26
$\{C_{10}^{(-4,2,2)}, W_1\}$	0.02215	0.3080	0.4754	1.072	1.945	0.4044	29.46	30.69	57.85	29.93	30.75
$\{C_{10}^{(-4,4,-4)}, W_1\}$	0.02373	0.3086	0.5177	1.109	1.192	0.2251	20.42	22.16	53.86	10.27	22.32
$\{C_{10}^{(-2,-4,-4)}, W_1\}$	0.02251	0.3321	0.4791	1.269	0.8273	0.1351	18.79	20.66	53.32	7.269	20.81
$\{C_{10}^{(-2,-2,-4)}, W_1\}$	0.02255	0.3321	0.4803	0.7465	1.183	1.883	18.82	20.69	53.32	7.488	20.84
$\{C_{10}^{(-2,-2,-4)}, W_3\}$	0.02200	0.3068	0.5357	1.085	1.311	0.2429	26.76	28.11	56.53	16.09	28.16
$\{C_{10}^{(-2,-2,-2)}, W_3\}$	0.02200	0.3068	0.5357	1.085	1.164	0.1306	23.64	25.15	55.12	11.34	25.21
$\{C_{10}^{(-2,-2,2)}, W_1\}$	0.02219	0.3077	0.4845	1.501	0.08102	0.4909	29.94	31.15	58.11	29.31	31.20
$\{C_{10}^{(-2,-2,2)}, W_3\}$	0.02215	0.3081	0.4985	1.457	0.6427	0.8948	22.73	24.30	54.74	14.92	24.37
$\{C_{10}^{(-2,0,-4)}, W_1\}$	0.02251	0.3321	0.4792	1.269	0.8271	0.1349	18.79	20.66	53.32	7.271	20.81
$\{C_{10}^{(-2,0,-2)}, W_1\}$	0.02353	0.3113	0.4442	1.363	1.682	0.7209	23.30	24.84	54.53	21.98	24.95
$\{C_{10}^{(-2,0,0)}, W_1\}$	0.02215	0.3083	0.4697	1.234	0.6553	1.395	20.77	22.48	53.96	11.55	22.55
$\{C_{10}^{(-2,0,2)}, W_1\}$	0.02216	0.3082	0.4931	0.8190	0.04436	0.4637	29.91	31.12	58.07	28.49	31.18
$\{C_{10}^{(-2,2,-4)}, W_1\}$	0.02250	0.3321	0.4789	1.269	0.8274	0.1355	18.80	20.67	53.32	7.266	20.82
$\{C_{10}^{(-2,2,2)}, W_1\}$	0.02216	0.3080	0.4749	1.069	1.943	0.4021	29.37	30.60	57.81	29.81	30.66
$\{C_{10}^{(-2,4,-4)}, W_1\}$	0.02374	0.3092	0.5188	1.109	1.195	0.2286	20.42	22.15	53.86	10.31	22.32
$\{C_{10}^{(-2,4,2)}, W_1\}$	0.02216	0.3052	0.4897	1.555	1.379	1.291	16.93	18.99	52.51	11.37	19.06

Continued on next page

Table 4-continued from previous page

$\{C_m^{(k_1,k_2,k_3)}, W_j\}$	$\sin^2\theta_{13}$	$\sin^2\theta_{12}$	$\sin^2\theta_{23}$	$\delta_{\rm CP}/\pi$	α_{21}/π	α_{31}/π	m_1/meV	m_2/meV	m_3/meV	$m_{\beta\beta}$/meV	m_β/meV
$\{C_{10}^{(0,-2,2)}, W_1\}$	0.02220	0.3073	0.4845	1.501	0.08097	0.4912	29.94	31.15	58.10	29.32	31.21
$\{C_{10}^{(0,-2,2)}, W_3\}$	0.02215	0.3081	0.4985	1.457	1.017	1.013	18.69	20.57	53.19	7.577	20.65
$\{C_{10}^{(0,2,2)}, W_1\}$	0.02215	0.3081	0.4748	1.068	1.943	0.4018	29.36	30.59	57.81	29.80	30.65
$\{C_{10}^{(0,4,-4)}, W_1\}$	0.02359	0.3086	0.5213	1.111	1.197	0.2298	20.39	22.13	53.85	10.34	22.29
$\{C_{10}^{(2,-4,2)}, W_1\}$	0.02216	0.3080	0.4890	1.180	1.846	1.480	29.44	30.67	57.85	27.32	30.72
$\{C_{10}^{(2,-4,2)}, W_3\}$	0.02209	0.3081	0.5039	1.229	0.9490	1.984	20.62	22.34	53.90	7.408	22.41
$\{C_{10}^{(2,-2,-2)}, W_1\}$	0.02222	0.3063	0.5844	1.070	1.764	1.430	29.95	31.16	58.08	27.41	31.21
$\{C_{10}^{(2,-2,0)}, W_1\}$	0.02230	0.3069	0.5844	1.070	1.764	1.429	29.96	31.17	58.06	27.42	31.23
$\{C_{10}^{(2,-2,2)}, W_1\}$	0.02219	0.3077	0.4844	1.501	0.08108	0.4907	29.93	31.14	58.12	29.30	31.20
$\{C_{10}^{(2,-2,2)}, W_3\}$	0.02209	0.3081	0.5039	1.229	0.9300	1.970	20.58	22.30	53.88	7.417	22.37
$\{C_{10}^{(2,-2,4)}, W_1\}$	0.02236	0.3046	0.5842	1.068	1.764	1.427	29.99	31.20	58.01	27.44	31.25
$\{C_{10}^{(2,0,-4)}, W_1\}$	0.02216	0.3083	0.4697	1.090	1.153	0.1967	17.39	19.40	52.75	8.183	19.48
$\{C_{10}^{(2,0,-2)}, W_1\}$	0.02215	0.3139	0.4727	1.873	0.8193	1.697	21.41	23.07	54.23	10.24	23.15
$\{C_{10}^{(2,0,0)}, W_1\}$	0.02215	0.3083	0.4697	1.234	0.6554	1.395	20.77	22.48	53.96	11.55	22.55
$\{C_{10}^{(2,0,2)}, W_1\}$	0.02219	0.3056	0.5172	0.7277	0.1327	1.633	29.93	31.14	58.12	30.26	31.19
$\{C_{10}^{(2,0,2)}, W_3\}$	0.02210	0.3081	0.5039	1.229	0.4114	1.582	28.88	30.14	57.57	22.43	30.19
$\{C_{10}^{(2,0,4)}, W_1\}$	0.02216	0.3083	0.4698	1.090	1.153	0.1964	17.39	19.40	52.75	8.182	19.48
$\{C_{10}^{(2,2,2)}, W_1\}$	0.02215	0.3080	0.4746	1.067	1.943	0.4010	29.32	30.56	57.78	29.76	30.61
$\{C_{10}^{(2,2,2)}, W_3\}$	0.02209	0.3081	0.5039	1.229	0.5242	1.672	24.91	26.35	55.68	16.88	26.41
$\{C_{10}^{(2,4,-4)}, W_1\}$	0.02354	0.3112	0.5220	1.116	1.204	0.2378	20.38	22.12	53.81	10.38	22.28
$\{C_{10}^{(2,4,2)}, W_3\}$	0.02209	0.3081	0.5039	1.228	0.4102	1.581	28.95	30.20	57.60	22.51	30.25
$\{C_{10}^{(4,-2,2)}, W_1\}$	0.02220	0.3080	0.4844	1.501	0.08112	0.4910	29.94	31.15	58.11	29.31	31.20
$\{C_{10}^{(4,0,-4)}, W_1\}$	0.02215	0.3076	0.4710	1.007	0.5534	1.413	22.97	24.52	54.83	15.22	24.59
$\{C_{10}^{(4,0,-2)}, W_1\}$	0.02215	0.3076	0.4710	1.007	0.5534	1.413	22.96	24.52	54.83	15.22	24.59
$\{C_{10}^{(4,0,0)}, W_1\}$	0.02215	0.3083	0.4697	1.234	0.6553	1.395	20.77	22.48	53.96	11.55	22.55
$\{C_{10}^{(4,0,2)}, W_1\}$	0.02212	0.3088	0.4718	1.057	1.378	0.5226	22.11	23.72	54.50	13.75	23.79
$\{C_{10}^{(4,0,4)}, W_1\}$	0.02212	0.3088	0.4717	1.056	1.378	0.5227	22.11	23.72	54.51	13.76	23.79
$\{C_{10}^{(4,2,2)}, W_1\}$	0.02215	0.3080	0.4758	1.075	1.946	0.4059	29.53	30.75	57.89	30.01	30.81
$\{C_{10}^{(4,4,-4)}, W_1\}$	0.02372	0.3086	0.5172	1.109	1.191	0.2242	20.42	22.16	53.86	10.25	22.32
$\{C_{10}^{(4,4,0)}, W_1\}$	0.02261	0.3043	0.4412	1.947	0.6146	1.595	19.96	21.73	53.73	13.04	21.83

[33] corresponds to our model $\{C_{10}^{(-2,0,0)}, W_1\}$. This model does not appear in Table 6 for the IO case because it fails to satisfy the cosmological upper bound on the sum of neutrino masses $\sum_{i=1}^{3} m_i < 120\,\text{meV}$ which is enforced in our analysis.

In all these models, the modulus τ is regarded as a free parameter to maximize the agreement between theoretical predictions and experimental data. The best fit values of the complex modulus τ in the fundamental domain of SL(2,$\mathbb{Z}$) are displayed in Fig. 1. This analysis includes 194 viable models for the NO case (147 without CP and 47 with CP) and 11 models for the IO case (6 without CP and 5 with CP). Evidently, the VEVs of τ in most viable models cluster near the regions $\Re\tau = 0$, $|\tau| = 1$ or $\Re\tau = \pm 0.5$ for both the mass orderings. The key observables for each model, which include the three lepton mixing angles, three CP-violating phases, $\sum_{i=1}^{3} m_i$, $m_{\beta\beta}$, and m_β are relevant to their minimal χ^2 values. The corresponding results for the NO case are displayed in Figs. 2 and 4, and those for the IO cases are presented in Figs. 3 and 5. Only a few models feature the best fit values for all the three mixing angles and the Dirac CP phase within the experimental 1σ ranges, indicating strong agreement with data, as shown in Figs. 2 and 3. Next-generation neutrino oscillation experiments and cosmological surveys will facilitate precise measurements of the lepton mixing parameters and neutrino masses. Combined with the accurate determination of $m_{\beta\beta}$, the joint analysis of

Table 5. Best fit values of the input parameters, neutrino masses, and mixing parameters at the minimum χ^2 for viable models $\{C_m^{(k_1,k_2,k_3)}, W_j\}$ with gCP symmetry.

Models	Best fit results for 47 viable models $\{C_m^{(k_1,k_2,k_3)}, W_j\}$ with gCP							
$\{C_m^{(k_1,k_2,k_3)}, W_j\}$	$\Re\langle\tau\rangle$	$\Im\langle\tau\rangle$	β/α	γ/α	g_2/g_1	αv/MeV	$(g_1 v^2/\Lambda)$/meV	$\chi^2_{\rm min}$
$\{C_2^{(-4,-2,2)}, W_3\}$	−0.1123	1.107	1532.0	100.4	−3.292	1.925	175.4	5.904
$\{C_3^{(-4,-2,2)}, W_1\}$	−0.01204	1.082	248.3	882.9	−1.588	1.707	418.6	2.010
$\{C_4^{(-4,-2,-2)}, W_3\}$	0.3203	0.9639	65.85	1065.0	3.867	3.527	186.9	12.20
$\{C_4^{(-4,2,0)}, W_1\}$	−0.3678	0.9781	7.439	535.0	1.583	11.41	607.5	25.69
$\{C_4^{(-4,4,0)}, W_1\}$	0.4481	1.026	47.70	1768.0	2.086	3.302	406.1	1.796
$\{C_4^{(-2,0,-2)}, W_3\}$	0.3203	0.9637	0.007489	16.18	3.868	232.3	186.9	12.20
$\{C_4^{(-2,2,0)}, W_1\}$	−0.3679	0.9781	25.68	1846.0	1.583	3.307	607.5	25.69
$\{C_4^{(-2,4,0)}, W_1\}$	0.4483	1.027	15.92	590.9	2.085	9.873	405.4	1.746
$\{C_4^{(0,2,0)}, W_1\}$	−0.3679	0.9781	33.64	2418.0	1.583	2.525	607.5	25.67
$\{C_4^{(0,4,0)}, W_1\}$	0.4482	1.027	77.00	2857.0	2.085	2.042	405.5	1.764
$\{C_4^{(2,4,0)}, W_1\}$	0.4482	1.027	133.4	4950.0	2.084	1.179	405.5	1.786
$\{C_5^{(-4,-2,2)}, W_1\}$	−0.01142	1.036	180.5	781.3	−1.579	1.867	460.1	6.319
$\{C_5^{(-4,2,2)}, W_3\}$	−0.3158	0.9870	19.64	317.8	3.708	4.514	185.3	3.311
$\{C_5^{(-2,2,2)}, W_1\}$	−0.01137	1.063	9.863	145.9	−1.589	10.26	434.8	5.723
$\{C_5^{(0,2,2)}, W_1\}$	−0.01137	1.063	71.14	1052.0	−1.589	1.423	434.7	5.721
$\{C_5^{(2,4,2)}, W_3\}$	0.3158	0.9870	0.006438	16.18	3.708	88.65	185.3	6.372
$\{C_6^{(-4,0,2)}, W_1\}$	−0.3679	0.9781	2491.0	34.65	1.583	2.451	607.5	25.67
$\{C_6^{(-4,0,4)}, W_1\}$	0.4483	1.027	2475.0	66.71	2.085	2.357	405.5	1.757
$\{C_6^{(-2,0,2)}, W_1\}$	−0.3679	0.9782	1717.0	23.89	1.582	3.555	607.5	25.65
$\{C_6^{(-2,0,4)}, W_1\}$	0.4482	1.027	1233.0	33.22	2.085	4.732	405.5	1.784
$\{C_7^{(-2,2,0)}, W_3\}$	−0.1123	1.107	0.06553	0.0005474	−3.292	2949.0	175.4	5.905
$\{C_7^{(-2,2,2)}, W_3\}$	−0.3542	0.9644	0.002120	6.324	4.066	223.2	188.9	8.906
$\{C_7^{(-2,4,2)}, W_3\}$	0.2289	1.002	0.002344	6.993	3.709	205.8	171.0	5.994
$\{C_8^{(-4,2,2)}, W_1\}$	−0.01137	1.063	846.6	57.26	−1.589	1.767	434.7	5.721
$\{C_8^{(-2,2,-2)}, W_1\}$	−0.01142	1.036	90.13	20.81	−1.579	16.18	460.1	6.312
$\{C_8^{(-2,2,2)}, W_1\}$	−0.01137	1.063	65.45	4.421	−1.589	22.86	434.7	5.708
$\{C_8^{(0,2,2)}, W_1\}$	−0.01137	1.063	1037.0	70.15	−1.589	1.443	434.7	5.721
$\{C_9^{(-4,2,-2)}, W_3\}$	0.2289	1.002	500.8	71.62	3.710	2.874	171.0	5.993
$\{C_9^{(-2,2,-2)}, W_3\}$	0.2289	1.002	832.7	119.1	3.710	1.728	171.0	5.992
$\{C_9^{(0,2,-2)}, W_3\}$	0.2289	1.002	820.6	117.4	3.710	1.754	171.0	5.994
$\{C_9^{(2,4,-2)}, W_3\}$	0.2289	1.002	0.0002417	0.1430	3.710	1439.0	171.0	5.993
$\{C_{10}^{(-2,-2,-4)}, W_3\}$	0.3203	0.9636	16.18	0.03275	3.868	232.3	186.9	12.19
$\{C_{10}^{(-2,-2,-2)}, W_3\}$	0.3203	0.9637	16.18	0.005280	3.868	232.3	186.9	12.21
$\{C_{10}^{(-2,-2,2)}, W_3\}$	0.2289	1.002	34.05	238.1	3.710	6.044	171.0	5.991
$\{C_{10}^{(0,-2,2)}, W_3\}$	0.2289	1.002	134.1	937.8	3.710	1.535	171.0	5.993
$\{C_{10}^{(2,-4,2)}, W_3\}$	−0.3158	0.9870	0.02204	16.18	3.708	88.65	185.3	3.313
$\{C_{10}^{(2,-2,2)}, W_3\}$	−0.3159	0.9870	0.05133	16.19	3.708	88.63	185.3	3.315
$\{C_{10}^{(2,0,2)}, W_3\}$	−0.3158	0.9870	0.02714	16.18	3.708	88.65	185.3	3.312
$\{C_{10}^{(2,0,4)}, W_1\}$	0.3680	0.9788	71.78	0.004320	1.581	84.99	606.3	29.41

Continued on next page

Table 5-continued from previous page

Models	Best fit results for 47 viable models $\{C_m^{(k_1,k_2,k_3)}, W_j\}$ with gCP								
$\{C_m^{(k_1,k_2,k_3)}, W_j\}$	$\Re\langle\tau\rangle$	$\Im\langle\tau\rangle$	β/α	γ/α	g_2/g_1	αv/MeV	$(g_1 v^2/\Lambda)$/meV	$\chi^2_{\min}$	
$\{C_{10}^{(2,2,2)}, W_1\}$	−0.01137	1.063	0.01907	14.79	−1.589	101.2	434.7	5.719	
$\{C_{10}^{(2,2,2)}, W_3\}$	−0.3158	0.9870	0.005264	16.18	3.708	88.65	185.3	3.313	
$\{C_{10}^{(2,4,2)}, W_3\}$	−0.3158	0.9870	0.01080	16.18	3.708	88.64	185.3	3.309	
$\{C_{10}^{(4,0,-4)}, W_1\}$	−0.4482	1.026	37.08	0.02417	2.086	157.4	405.9	3.970	
$\{C_{10}^{(4,0,-2)}, W_1\}$	0.4481	1.026	37.07	0.006623	2.086	157.5	406.1	1.777	
$\{C_{10}^{(4,0,0)}, W_1\}$	0.4481	1.026	37.07	0.01429	2.086	157.5	406.1	1.786	
$\{C_{10}^{(4,0,2)}, W_1\}$	−0.4482	1.026	37.09	0.006124	2.086	157.4	405.9	3.967	
$\{C_{10}^{(4,0,4)}, W_1\}$	−0.4482	1.026	37.08	0.002308	2.086	157.4	405.9	3.976	
$\{C_m^{(k_1,k_2,k_3)}, W_j\}$	$\sin^2\theta_{13}$	$\sin^2\theta_{12}$	$\sin^2\theta_{23}$	$\delta_{\rm CP}/\pi$	α_{21}/π	α_{31}/π	m_1/meV	m_2/meV	m_3/meV	$m_{\beta\beta}$/meV	m_β/meV
$\{C_2^{(-4,-2,2)}, W_3\}$	0.02216	0.3108	0.4496	1.475	1.557	1.397	21.61	23.25	54.28	17.02	23.33
$\{C_3^{(-4,-2,2)}, W_1\}$	0.02215	0.3075	0.4790	1.371	1.635	1.757	19.99	21.76	53.65	16.20	21.83
$\{C_4^{(-4,-2,-2)}, W_3\}$	0.02203	0.3071	0.5358	1.086	0.9376	1.965	22.07	23.68	54.46	8.956	23.74
$\{C_4^{(-4,2,0)}, W_1\}$	0.02190	0.2951	0.4655	0.06093	1.026	0.1175	21.76	23.40	54.32	9.479	23.43
$\{C_4^{(-4,4,0)}, W_1\}$	0.02177	0.3156	0.4871	1.161	1.357	0.5021	21.24	22.91	54.38	13.43	22.99
$\{C_4^{(-2,0,-2)}, W_3\}$	0.02200	0.3068	0.5357	1.085	0.9383	1.965	22.08	23.69	54.47	8.970	23.75
$\{C_4^{(-2,2,0)}, W_1\}$	0.02190	0.2951	0.4655	0.06084	1.026	0.1176	21.76	23.40	54.32	9.477	23.43
$\{C_4^{(-2,4,0)}, W_1\}$	0.02182	0.3147	0.4886	1.161	1.356	0.5002	21.21	22.88	54.36	13.40	22.96
$\{C_4^{(0,2,0)}, W_1\}$	0.02190	0.2952	0.4655	0.06093	1.026	0.1177	21.76	23.39	54.32	9.474	23.43
$\{C_4^{(0,4,0)}, W_1\}$	0.02182	0.3148	0.4887	1.160	1.356	0.5003	21.21	22.88	54.36	13.40	22.96
$\{C_4^{(2,4,0)}, W_1\}$	0.02182	0.3148	0.4888	1.160	1.356	0.5003	21.20	22.88	54.36	13.40	22.96
$\{C_5^{(-4,-2,2)}, W_1\}$	0.02217	0.3079	0.4932	1.495	1.936	1.955	17.32	19.34	52.72	16.30	19.42
$\{C_5^{(-4,2,2)}, W_3\}$	0.02209	0.3081	0.5039	1.228	0.8950	1.945	20.54	22.27	53.87	7.571	22.34
$\{C_5^{(-2,2,2)}, W_1\}$	0.02217	0.3074	0.4892	1.491	1.755	1.822	18.71	20.59	53.20	16.51	20.67
$\{C_5^{(0,2,2)}, W_1\}$	0.02217	0.3074	0.4892	1.491	1.755	1.822	18.71	20.59	53.20	16.51	20.67
$\{C_5^{(2,4,2)}, W_3\}$	0.02208	0.3081	0.5039	0.7716	1.105	0.05495	20.55	22.27	53.87	7.571	22.34
$\{C_6^{(-4,0,2)}, W_1\}$	0.02190	0.2952	0.4655	0.06092	1.026	0.1178	21.76	23.39	54.32	9.474	23.43
$\{C_6^{(-4,0,4)}, W_1\}$	0.02182	0.3148	0.4886	1.160	1.356	0.5002	21.21	22.88	54.36	13.40	22.96
$\{C_6^{(-2,0,2)}, W_1\}$	0.02190	0.2953	0.4655	0.06096	1.026	0.1179	21.76	23.39	54.32	9.470	23.43
$\{C_6^{(-2,0,4)}, W_1\}$	0.02182	0.3148	0.4888	1.160	1.356	0.5003	21.20	22.88	54.36	13.40	22.96
$\{C_7^{(-2,2,0)}, W_3\}$	0.02216	0.3108	0.4496	1.475	1.557	1.397	21.60	23.25	54.28	17.02	23.33
$\{C_7^{(-2,2,2)}, W_3\}$	0.02216	0.3080	0.4983	1.551	1.015	0.008529	23.75	25.26	55.17	7.306	25.33
$\{C_7^{(-2,4,2)}, W_3\}$	0.02215	0.3081	0.4985	1.457	1.014	1.012	18.69	20.57	53.19	7.577	20.65
$\{C_8^{(-4,2,2)}, W_1\}$	0.02217	0.3074	0.4892	1.491	1.755	1.822	18.71	20.59	53.20	16.51	20.67
$\{C_8^{(-2,2,-2)}, W_1\}$	0.02217	0.3079	0.4932	1.495	1.936	1.955	17.32	19.34	52.72	16.30	19.42
$\{C_8^{(-2,2,2)}, W_1\}$	0.02217	0.3074	0.4892	1.490	1.755	1.821	18.72	20.60	53.21	16.51	20.68
$\{C_8^{(0,2,2)}, W_1\}$	0.02217	0.3074	0.4892	1.491	1.755	1.822	18.71	20.59	53.20	16.51	20.67
$\{C_9^{(-4,2,-2)}, W_3\}$	0.02215	0.3081	0.4985	1.457	1.014	1.012	18.69	20.57	53.19	7.576	20.65
$\{C_9^{(-2,2,-2)}, W_3\}$	0.02215	0.3081	0.4985	1.457	1.014	1.012	18.69	20.57	53.19	7.575	20.65
$\{C_9^{(0,2,-2)}, W_3\}$	0.02215	0.3081	0.4985	1.457	1.014	1.012	18.69	20.57	53.19	7.576	20.65
$\{C_9^{(2,4,-2)}, W_3\}$	0.02215	0.3081	0.4985	1.457	1.014	1.012	18.69	20.57	53.19	7.576	20.65

Continued on next page

Table 5-continued from previous page

$\{C_m^{(k_1,k_2,k_3)}, W_j\}$	$\sin^2\theta_{13}$	$\sin^2\theta_{12}$	$\sin^2\theta_{23}$	$\delta_{\rm CP}/\pi$	α_{21}/π	α_{31}/π	m_1/meV	m_2/meV	m_3/meV	$m_{\beta\beta}$/meV	m_β/meV
$\{C_{10}^{(-2,-2,-4)}, W_3\}$	0.02200	0.3068	0.5357	1.085	0.9387	1.965	22.08	23.69	54.47	8.972	23.75
$\{C_{10}^{(-2,-2,-2)}, W_3\}$	0.02200	0.3068	0.5357	1.085	0.9383	1.965	22.08	23.69	54.47	8.970	23.75
$\{C_{10}^{(-2,-2,2)}, W_3\}$	0.02215	0.3081	0.4985	1.457	1.014	1.012	18.69	20.57	53.19	7.575	20.65
$\{C_{10}^{(0,-2,2)}, W_3\}$	0.02215	0.3081	0.4985	1.457	1.014	1.012	18.69	20.57	53.19	7.576	20.65
$\{C_{10}^{(2,-4,2)}, W_3\}$	0.02209	0.3081	0.5039	1.229	0.8950	1.945	20.54	22.27	53.87	7.570	22.34
$\{C_{10}^{(2,-2,2)}, W_3\}$	0.02209	0.3081	0.5039	1.229	0.8950	1.945	20.54	22.27	53.87	7.569	22.34
$\{C_{10}^{(2,0,2)}, W_3\}$	0.02209	0.3081	0.5039	1.229	0.8950	1.945	20.54	22.27	53.87	7.570	22.34
$\{C_{10}^{(2,0,4)}, W_1\}$	0.02185	0.2951	0.4672	1.938	0.9735	1.881	21.71	23.35	54.28	9.457	23.38
$\{C_{10}^{(2,2,2)}, W_1\}$	0.02217	0.3074	0.4892	1.491	1.755	1.822	18.71	20.59	53.20	16.51	20.67
$\{C_{10}^{(2,2,2)}, W_3\}$	0.02209	0.3081	0.5039	1.229	0.8950	1.945	20.54	22.27	53.87	7.571	22.34
$\{C_{10}^{(2,4,2)}, W_3\}$	0.02209	0.3081	0.5039	1.228	0.8950	1.945	20.54	22.27	53.87	7.571	22.34
$\{C_{10}^{(4,0,-4)}, W_1\}$	0.02178	0.3152	0.4874	0.8391	0.6438	1.499	21.23	22.91	54.37	13.42	22.98
$\{C_{10}^{(4,0,-2)}, W_1\}$	0.02178	0.3156	0.4870	1.161	1.357	0.5021	21.24	22.91	54.38	13.43	22.99
$\{C_{10}^{(4,0,0)}, W_1\}$	0.02178	0.3156	0.4870	1.161	1.357	0.5021	21.24	22.91	54.38	13.43	22.99
$\{C_{10}^{(4,0,2)}, W_1\}$	0.02178	0.3151	0.4874	0.8391	0.6438	1.499	21.23	22.91	54.37	13.42	22.98
$\{C_{10}^{(4,0,4)}, W_1\}$	0.02178	0.3152	0.4874	0.8391	0.6438	1.499	21.23	22.91	54.37	13.42	22.98

Table 6. Best fit values of the input parameters, neutrino masses, and mixing parameters at the minimum χ^2 for viable models $\{C_m^{(k_1,k_2,k_3)}, W_j\}$ without gCP symmetry.

Models	Best fit results for 6 viable models $\{C_m^{(k_1,k_2,k_3)}, W_j\}$ without gCP								
$\{C_m^{(k_1,k_2,k_3)}, W_j\}$	$\Re\langle\tau\rangle$	$\Im\langle\tau\rangle$	β/α	γ/α	$\lvert g_2/g_1\rvert$	$\arg(g_2/g_1)/\pi$	αv/MeV	$(g_1 v^2/\Lambda)$/meV	$\chi^2_{\rm min}$
$\{C_7^{(-4,-2,-4)}, W_3\}$	−0.418	1.05	1794.0	186.6	42.8	1.57	1.74	20.5	8.27
$\{C_7^{(-4,-2,2)}, W_3\}$	0.459	1.06	108.0	843.3	19.5	0.523	1.67	44.1	12.2
$\{C_7^{(-2,2,-4)}, W_3\}$	−0.418	1.05	0.000155	0.104	13.3	1.52	3123.0	65.8	8.27
$\{C_9^{(-4,2,-2)}, W_3\}$	−0.418	1.05	0.00591	9.62	32.4	0.447	324.7	27.0	8.29
$\{C_9^{(2,4,-2)}, W_3\}$	0.459	1.06	0.000254	0.128	9.10	0.511	1408.0	94.6	12.2
$\{C_{10}^{(2,4,2)}, W_3\}$	0.388	1.10	76.5	1414.0	14.3	0.636	1.02	56.2	2.50
$\{C_m^{(k_1,k_2,k_3)}, W_j\}$	$\sin^2\theta_{13}$	$\sin^2\theta_{12}$	$\sin^2\theta_{23}$	δ_{CP}/π	α_{21}/π	α_{31}/π	m_1/meV	m_2/meV	m_3/meV	$m_{\beta\beta}$/meV	m_β/meV
$\{C_7^{(-4,-2,-4)}, W_3\}$	0.02240	0.311	0.509	1.40	0.766	1.42	49.1	49.9	2.08	24.1	48.8
$\{C_7^{(-4,-2,2)}, W_3\}$	0.02231	0.308	0.499	1.60	1.06	0.645	49.3	50.0	4.72	18.7	49.0
$\{C_7^{(-2,2,-4)}, W_3\}$	0.02240	0.311	0.509	1.40	0.708	1.32	49.5	50.3	6.59	27.0	49.2
$\{C_9^{(-4,2,-2)}, W_3\}$	0.02240	0.311	0.509	1.40	0.826	0.289	49.2	49.9	2.72	21.6	48.8
$\{C_9^{(2,4,-2)}, W_3\}$	0.02231	0.308	0.499	1.60	1.12	0.615	50.0	50.8	9.61	20.5	49.7
$\{C_{10}^{(2,4,2)}, W_3\}$	0.02232	0.309	0.548	1.30	0.772	0.664	50.0	50.7	9.27	24.6	49.6

these experimental data will offer crucial evidence for investigating various modular models. Assuming that the current best fit value for $\sin^2\theta_{12}$ remains unchanged, this parameter will be measured with high precision after six years of data collection in the next-generation JUNO experiment. As shown in Figs. 2 and 3, its projected 3σ uncertainty range is sufficiently wide to encompass the predicted $\sin^2\theta_{12}$ values of almost all the models considered in this study. Distinguishing these modular models will require improved precision on θ_{23} and $\delta_{\rm CP}$. Future long baseline experiments DUNE [64] and T2HK [70] will critically test viable modular models through precision

Table 7. Best fit values of the input parameters, neutrino masses, and mixing parameters at the minimum χ^2 for viable models $\{C_m^{(k_1,k_2,k_3)}, W_j\}$ with gCP symmetry.

Models	Best fit results for 5 viable models $\{C_m^{(k_1,k_2,k_3)}, W_j\}$ with gCP							
$\{C_m^{(k_1,k_2,k_3)}, W_j\}$	$\Re\langle\tau\rangle$	$\Im\langle\tau\rangle$	β/α	γ/α	g_2/g_1	αv/MeV	$(g_1 v^2/\Lambda)$/meV	$\chi^2_{\rm min}$
$\{C_7^{(-4,-2,-4)}, W_3\}$	−0.418	1.05	1794.0	186.6	197.1	1.74	4.44	8.27
$\{C_7^{(-4,-2,2)}, W_3\}$	0.459	1.06	108.0	843.3	−266.3	1.67	3.23	12.2
$\{C_9^{(-4,2,-2)}, W_3\}$	−0.418	1.05	0.00591	9.62	197.3	324.7	4.44	8.29
$\{C_9^{(2,4,-2)}, W_3\}$	−0.459	1.05	0.00428	37.5	10000.0	82.6	0.0869	26.3
$\{C_{10}^{(2,4,2)}, W_3\}$	0.388	1.10	76.5	1414.0	−34.6	1.02	23.3	2.50

$\{C_m^{(k_1,k_2,k_3)}, W_j\}$	$\sin^2\theta_{13}$	$\sin^2\theta_{12}$	$\sin^2\theta_{23}$	$\delta_{\rm CP}/\pi$	α_{21}/π	α_{31}/π	m_1/meV	m_2/meV	m_3/meV	$m_{\beta\beta}$/meV	m_β/meV
$\{C_7^{(-4,-2,-4)}, W_3\}$	0.02240	0.311	0.509	1.40	0.792	1.84	49.1	49.8	0.576	23.0	48.8
$\{C_7^{(-4,-2,2)}, W_3\}$	0.02231	0.308	0.499	1.60	1.00	0.997	49.1	49.9	1.73	18.3	48.8
$\{C_9^{(-4,2,-2)}, W_3\}$	0.02240	0.311	0.509	1.40	0.792	1.84	49.1	49.8	0.574	23.0	48.8
$\{C_9^{(2,4,-2)}, W_3\}$	0.02232	0.295	0.476	1.40	0.998	0.991	49.1	49.8	0.731	19.5	48.7
$\{C_{10}^{(2,4,2)}, W_3\}$	0.02232	0.309	0.548	1.30	0.707	0.817	49.7	50.4	7.73	27.4	49.4

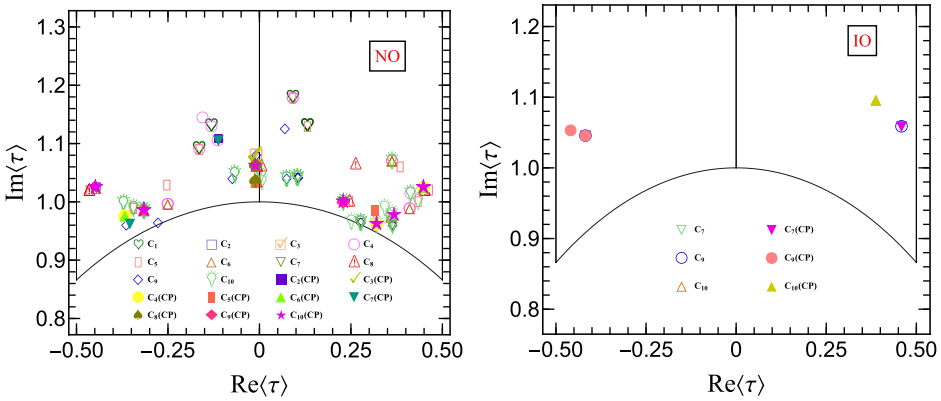

Fig. 1. (color online) Best fit values of the modulus τ for 147 (47) and six (five) viable models in the case without (with) gCP symmetry for the NO and IO neutrino mass spectra, respectively.

measurements of θ_{23} and $\delta_{\rm CP}$. The projected angular resolution of these parameters in DUNE, after 15 years of operation, is also shown in these two figures. Evidently, once DUNE and T2HK achieve their target sensitivity, the majority of the currently viable models will be decisively tested. The combination of JUNO, DUNE, and T2HK will provide a powerful approach for testing these models. Given the projected constraints from these experiments, only a small number of models provide results consistent with experimental data, whereas the vast majority is disfavored.

Figures 4 and 5 indicate that the predicted sum of neutrino masses $\sum_{i=1}^3 m_i$ for all the viable models lies within the detection range of future cosmological surveys. These estimates lie within the projected 1σ sensitivity $\sum_{i=1}^3 m_i < (44-76)$ meV of the combined Euclid+CMB-S4+LiteBIRD analysis [65], which assumes a fiducial $\sum_{i=1}^3 m_i = 60$ meV with a 1σ uncertainty of 16 meV. Notably, the minimal $\sum_{i=1}^3 m_i$ values obtained from oscillation data are approximately 59 meV (NO) and 99 meV (IO). The forecast $\sum_{i=1}^3 m_i < (44-76)$ meV is a sensitivity reach: achieving it would exclude IO, and for NO, it indicates masses close to the minimal values. As shown in Figs. 4 and 5, the lower bounds on the lightest neutrino mass $m_{\rm lightest}$ are derived from the cosmological limit $\sum_{i=1}^3 m_i < 120$ meV [61] combined with the measured mass squared differences. For NO, with $m_{\rm lightest} = m_1$,

$$m_2 = \sqrt{m_1^2 + \Delta m_{21}^2}, \quad m_3 = \sqrt{m_1^2 + \Delta m_{31}^2}, \tag{13}$$

using $\Delta m_{21}^2 = 7.49\times10^{-5}$ eV^2 and $\Delta m_{31}^2 = 2.513\times10^{-3}$ eV^2 gives $m_1 < 39.989$ meV. For IO, with $m_{\rm lightest} = m_3$,

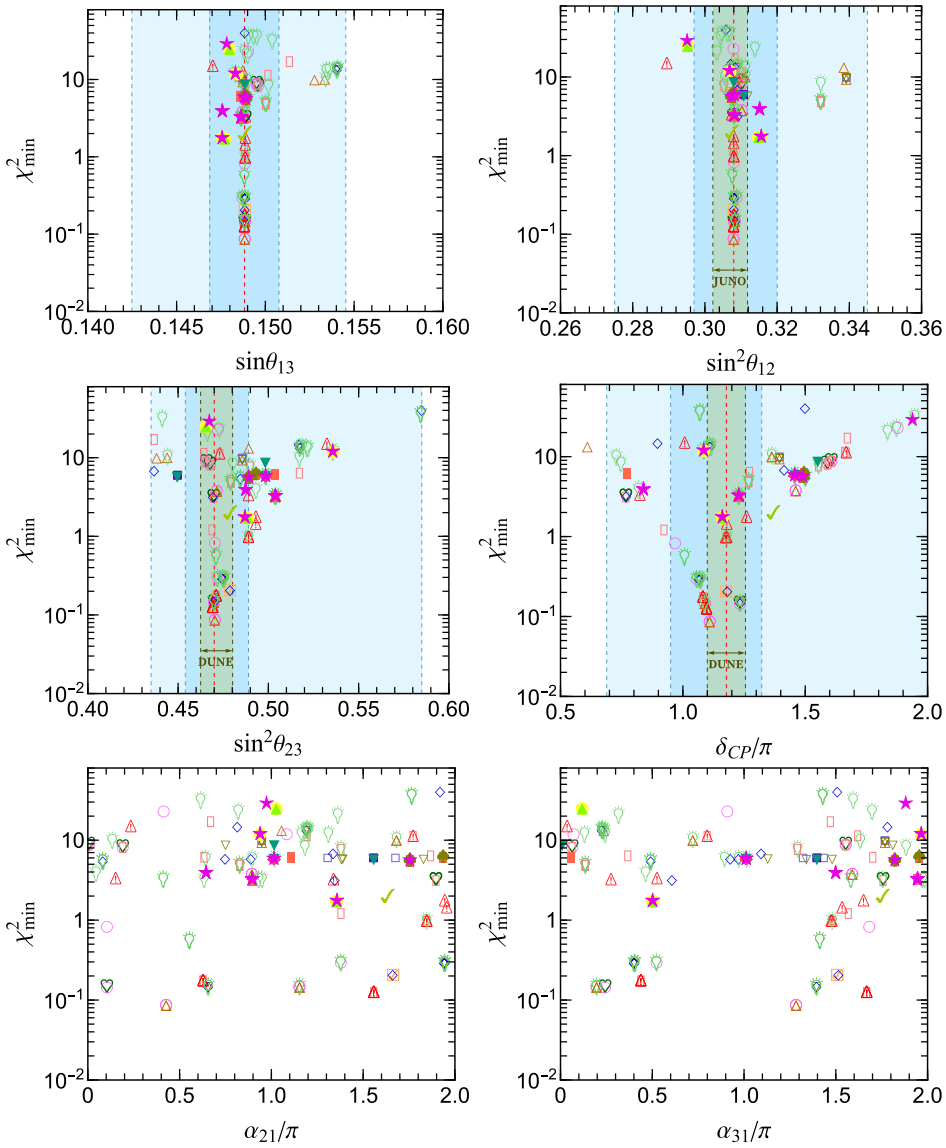

Fig. 2. (color online) Best fit values of the minimum value of χ^2. The three lepton mixing angles and three CP-violating phases for the viable models without (147 models) and with (47 models) gCP symmetry in the NO case. The red dashed lines in the first four panels represent the best fit values, and the light blue bounds represent the 1σ and 3σ ranges obtained from NuFIT 6.0 with Super-Kamiokande atmospheric data [62]. The lighter green band in the panel of $\sin^2\theta_{12}$ is the prospective 3σ range after six years of JUNO running [63]. The lighter green regions in the panels of $\sin^2\theta_{23}$ and $\delta_{\rm CP}$ are the resolution (in degrees) of the true values (corresponding to their best fit values given by NuFIT 6.0) after 15 years of DUNE running [64].

$$m_1 = \sqrt{m_3^2 - \Delta m_{32}^2 - \Delta m_{21}^2}, \quad m_2 = \sqrt{m_3^2 - \Delta m_{32}^2}, \tag{14}$$

using $\Delta m_{32}^2 = -2.484\times10^{-3}\ {\rm eV}^2$ yields $m_3 < 39.980$ meV. For the NO case, all the viable models yield m_β values below the forecasted detection limit of 0.04 eV reported by Project 8 [66], whereas for the IO case, m_β lies above this threshold. Predictions for $m_{\beta\beta}$ in all the viable NO models are compatible with the current KamLAND-Zen constraint of $m_{\beta\beta} < (28-122)$ meV [67], although this bound is expected to accommodate some viable IO models. Upcoming experiments such as LEGEND-1000 (aiming for $m_{\beta\beta} < (9\sim21)$ meV) [68] and nEXO (with a projected reach of $m_{\beta\beta} < (4.7\sim20.3)$ meV) [69] will be sufficiently sensitive to test most of the NO models and all the IO models. The relationship between the lightest neutrino mass (m_1 or m_3) and $m_{\beta\beta}$ for each viable case is illustrated in Figs. 4 and 5, highlighting parameter trends across mass orderings.

III. TYPICAL MODEL

Based on the aforementioned discussion, we have identified 147 (47) minimal phenomenologically viable

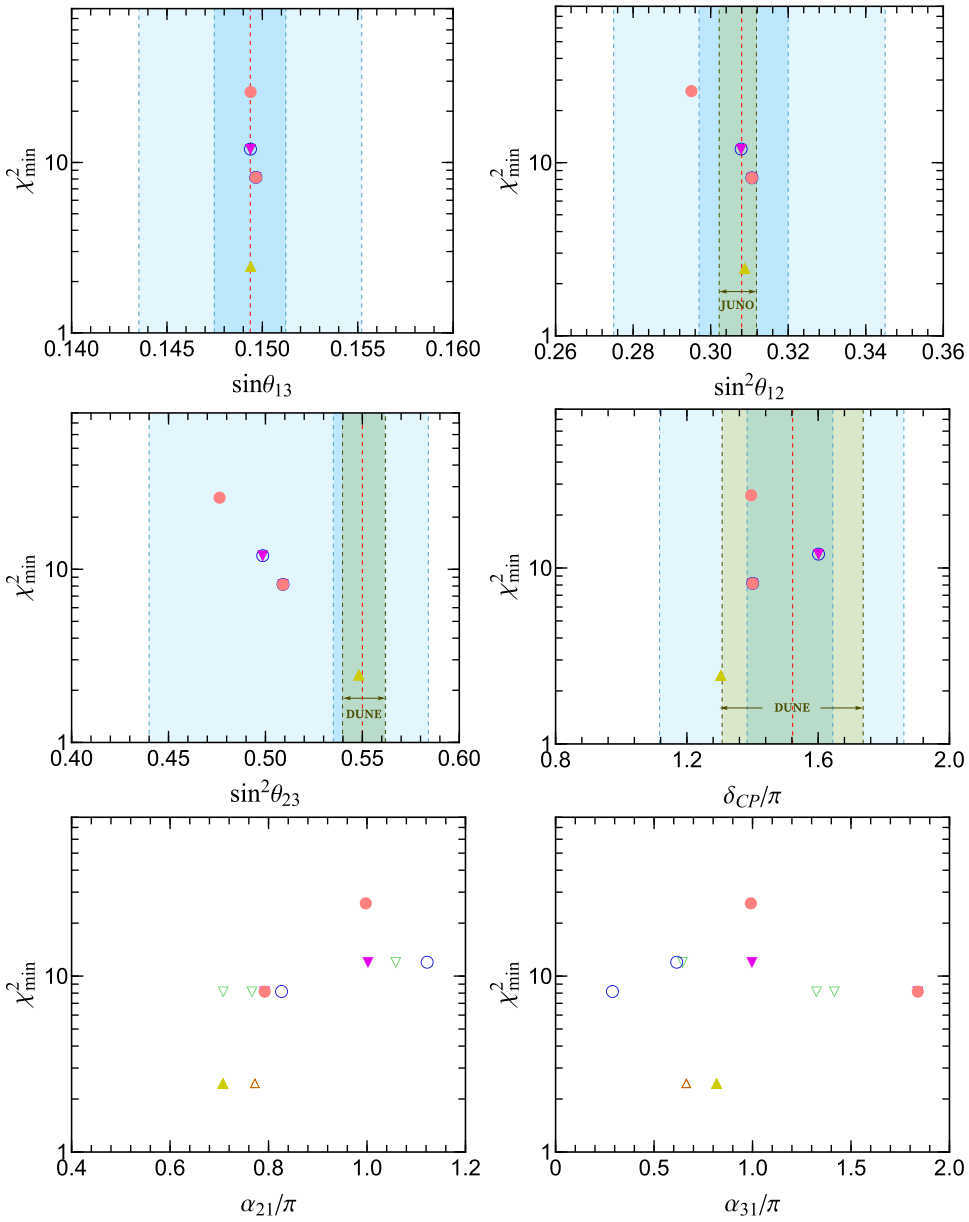

Fig. 3. (color online) Best fit values of the minimum value of χ^2. The three lepton mixing angles and three CP-violating phases for all the viable models without and with gCP symmetry in the IO case are shown.

lepton flavor models for the NO case and six (five) models for the IO case;they are constructed using level 3 polyharmonic polyharmonic Maaß with even weights, associated with the finite modular group $\Gamma_3 \cong A_4$ without (with) gCP symmetry. All these models are characterized by six real parameters αv, β/α, γ/α, $g_1 v^2/\Lambda$, $|g_2/g_1|$, and $\Im\tau$, along with two phases $\mathrm{Arg}(g_2/g_1)$ and $\Re\tau$, when gCP symmetry is not imposed. If gCP symmetry is present, then $\Re\tau$ serves as the only phase parameter. The three real values αv, β/α, and γ/α are determined by fitting the three charged lepton masses. Then, the remaining three real parameters and two (or one) phases determine the neutrino sector observables: the three neutrino masses, three mixing angles, Dirac CP-violating phase, and two Majorana CP-violating phases entering the PMNS matrix. Because nine neutrino observables are constrained by only five (or four) independent parameters, these non-holomorphic A_4 modular models are highly predictive. Consequently, the observables inevitably show non-trivial correlations, which can be derived through an analysis analogous to those presented in Refs. [18, 59]. A comprehensive analysis and complete graphical examination of all the viable models lie beyond the scope of the present study. To demonstrate the predictive efficacy of the non-holomorphic A_4 modular invariant models, we focus on a representative model that effectively illustrates the qual-

ity of the obtained results. Next, we present the detailed numerical results obtained for the model $\{C_{10}^{(2,4,2)}, W_3\}$ as illustrative examples. The representation and weight assignments for the lepton fields in this model are as follows:

$$\begin{aligned} &L \sim \mathbf{3}, \quad E_1^c \sim \mathbf{1}, \quad E_2^c \sim \mathbf{1}', \quad E_3^c \sim \mathbf{1}'', \\ &k_L = 0, \quad k_{E_1^c} = k_{E_3^c} = 2, \quad k_{E_2^c} = 4. \end{aligned} \tag{15}$$

The resulting charged lepton and light neutrino mass matrices can be obtained from Table 2 and Eq. (6) respectively:

$$M_e = \begin{pmatrix} \alpha Y_{\mathbf{3},1}^{(2)} & \alpha Y_{\mathbf{3},3}^{(2)} & \alpha Y_{\mathbf{3},2}^{(2)} \\ \beta Y_{\mathbf{3},3}^{(4)} & \beta Y_{\mathbf{3},2}^{(4)} & \beta Y_{\mathbf{3},1}^{(4)} \\ \gamma Y_{\mathbf{3},2}^{(2)} & \gamma Y_{\mathbf{3},1}^{(2)} & \gamma Y_{\mathbf{3},3}^{(2)} \end{pmatrix} v,$$

$$M_\nu = \frac{v^2}{2\Lambda} \begin{pmatrix} g_1 Y_{\mathbf{1}}^{(0)} + 2g_2 Y_{\mathbf{3},1}^{(0)} & -g_2 Y_{\mathbf{3},3}^{(0)} & -g_2 Y_{\mathbf{3},2}^{(0)} \\ -g_2 Y_{\mathbf{3},3}^{(0)} & 2g_2 Y_{\mathbf{3},2}^{(0)} & g_1 Y_{\mathbf{1}}^{(0)} - g_2 Y_{\mathbf{3},1}^{(0)} \\ -g_2 Y_{\mathbf{3},2}^{(0)} & g_1 Y_{\mathbf{1}}^{(0)} - g_2 Y_{\mathbf{3},1}^{(0)} & 2g_2 Y_{\mathbf{3},3}^{(0)} \end{pmatrix}, \tag{16}$$

where the explicit matrix elements are determined by polyharmonic Maaß forms of respective weights. This model can produce results consistent with the experimental data for both the NO and IO mass spectra under both conditions of with and without gCP symmetry. The predicted best fit values of the input parameters and physical observable quantities are summarized in Tables 4, 5, 6, and 7.

Performing exhaustive scans of the model's parameter spaces, while ensuring that all observables remain

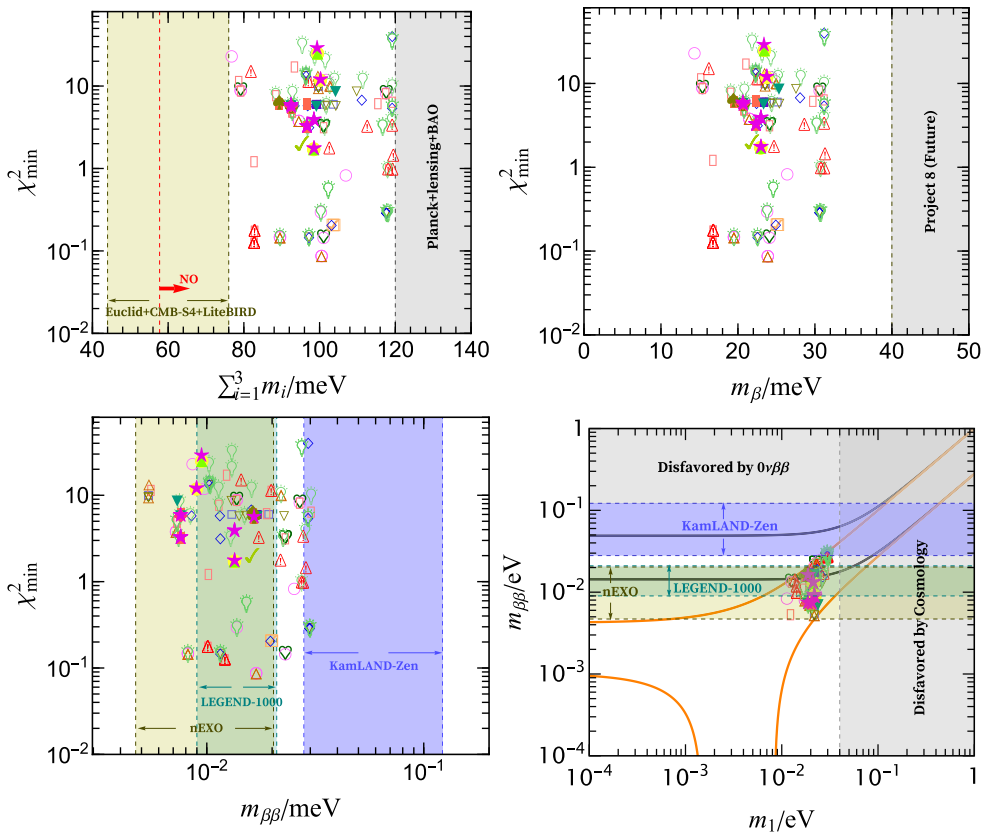

Fig. 4. (color online) Best fit values of the minimum value of χ^2, effective mass $m_{\beta\beta}$ in $0\nu\beta\beta$-decay, kinematical mass m_β in beta decay, and three neutrino mass sum $\sum_{i=1}^3 m_i$ are shown. In the panel of the neutrino mass sum $\sum_{i=1}^3 m_i$, the vertical bands indicate the current most stringent limit $\sum_{i=1}^3 m_i < 120\,\text{meV}$ from the Planck + lensing + BAO model [61]. The next-generation experiments sensitivity ranges $\sum_{i=1}^3 m_i < (44-76)\,\text{meV}$ of Euclid+CMB-S4+LiteBIRD [65] are shown. The red dashed line represents the limitation of the NO case ($\sum_{i=1}^3 m_i \geq 57.75\,\text{meV}$). In the panel of the kinematical mass m_β in beta decay, the gray region represents Project 8 future bound ($m_\beta < 0.04\,\text{meV}$) [66]. In the panel of the effective Majorana mass $m_{\beta\beta}$, the vertical bands indicate the latest result $m_{\beta\beta} < (28-122)\,\text{meV}$ of KamLAND-Zen [67] as well as the next-generation experimental sensitivity ranges $m_{\beta\beta} < (9-21)\,\text{meV}$ and $m_{\beta\beta} < (4.7-20.3)\,\text{meV}$ from LEGEND-1000 [68] and nEXO [69], respectively.

within their experimental 3σ ranges from NuFIT [58], reveals that the three lepton mixing angles and three CP violation phases are constrained within narrow ranges for both the mass hierarchies:

$$\begin{aligned}
\text{NO}:\ & \sin^2\theta_{13}\in[0.02030,0.02388]([0.02030,0.02388]), \quad \sin^2\theta_{12}\in[0.275,0.345]([0.296,0.340]),\\
& \sin^2\theta_{23}\in[0.501,0.506]([0.501,0.506]), \quad \delta_{\rm CP}/\pi\in[1.211,1.244]([1.211,1.242]),\\
& \alpha_{21}/\pi\in[0.368,1.419]([0.883,0.908]), \quad \alpha_{31}/\pi\in[-0.451,0.342]([-0.0628,-0.0455]),\\
& \sum_{i=1}^{3}m_i\in[94.20\,\text{meV},120\,\text{meV}]([94.29\,\text{meV},99.61\,\text{meV}]), \quad m_{\beta\beta}\in[5.673\,\text{meV},24.36\,\text{meV}]([6.068\,\text{meV},8.417\,\text{meV}]),\\
\text{IO}:\ & \sin^2\theta_{13}\in[0.0212,0.0234]([0.0212,0.0234]), \quad \sin^2\theta_{12}\in[0.301,330]([0.301,330]),\\
& \sin^2\theta_{23}\in[0.544,0.555]([0.544,0.554]), \quad \delta_{\rm CP}/\pi\in[1.301,1.311]([1.301,1.311]),\\
& \alpha_{21}/\pi\in[0.524,0.891]([0.692,0.719]), \quad \alpha_{31}/\pi\in[0.566,1.066]([0.811,0.823]),\\
& \sum_{i=1}^{3}m_i\in[105.8\,\text{meV},120\,\text{meV}]([105.8\,\text{meV},110.8\,\text{meV}]), \quad m_{\beta\beta}\in[20.56\,\text{meV},36.85\,\text{meV}]([26.29\,\text{meV},28.15\,\text{meV}]),
\end{aligned} \tag{17}$$

for the model $\{C_{10}^{(2,4,2)},W_3\}$ without (with) gCP symmetry. Remarkably, the atmospheric mixing angle θ_{23} well aligjns with its maximal value for NO case. When gCP symmetry compatible with the A_4 modular symmetry is

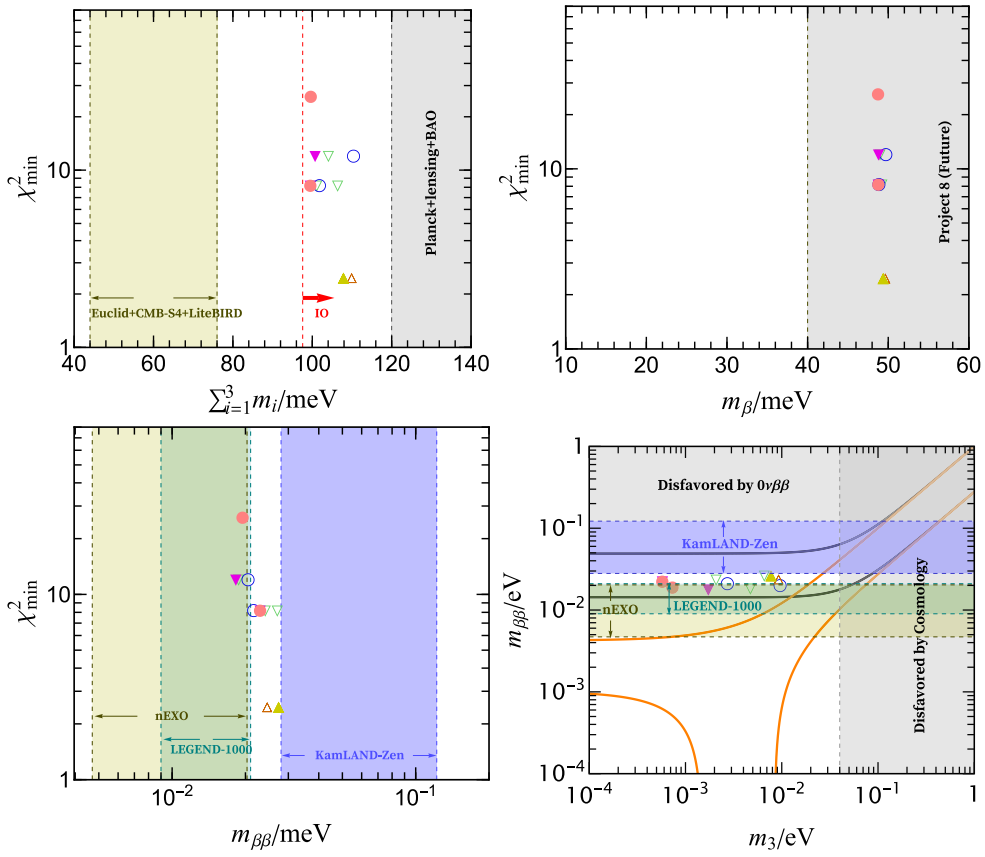

Fig. 5. (color online) Best fit values of the minimum value of χ^2, effective mass $m_{\beta\beta}$, kinematical mass m_β, and mass sum $\sum_{i=1}^{3}m_i$ are shown.

imposed, all the CP-violating phases are confined to narrow intervals, because gCP invariance requires all couplings to be real. This result indicates that CP violation can only arise from $\Re\tau$. Additionally, the Majorana CP phases α_{21} and α_{31} deviate slightly from their trivial values. These precise constraints imply that the model can be tested experimentally at the upcoming long baseline neutrino facilities DUNE and T2HK, which are highly sensitive to the Dirac CP-violating phase and atmospheric mixing angle. The neutrino mass parameters $\sum_{i=1}^{3} m_i$ and $m_{\beta\beta}$ are constrained across both the mass orderings. For the NO case, $\sum_{i=1}^{3} m_i$ falls in the sensitivity reach of upcoming cosmological surveys such as Euclid+CMB-S4+LiteBIRD. In contrast, while $m_{\beta\beta}$ lies below the current KamLAND-Zen limit, it can become accessible to next-generation experiments such as LEGEND-1000 and nEXO. Conversely, for the IO case, both the parameters lie within the projected detection ranges of future experiments, offering a clear avenue to distinguish between mass orderings.

Furthermore, we identify several notable correlations between the input parameters and physical observables. Specifically, distinct dependencies are observed between $\Re\tau$ and $\Im\tau$ as well as between the Dirac CP phase $\delta_{\rm CP}$ and $\Re\tau$. These correlations are separately illustrated for the NO and IO mass spectra in Figs. 6 and 7, respectively, where the green (red) points represent the results obtained without (with) imposing the gCP symmetry. Among the mixing observables, correlations are established between $\sin^2\theta_{23}$ and $\sin^2\theta_{13}$, $\sin^2\theta_{12}$, $\delta_{\rm CP}$, and the Majorana phase α_{21} (see Figs. 6 and 7 for the NO and IO cases, respectively). Notably, θ_{23} is strongly correlated with the other mixing parameters, in particular with the parameters fixed by the gCP symmetry. Moreover, a strong correlation exists between the Dirac CP phase $\delta_{\rm CP}$ and solar mixing angle θ_{12}. Such predicted interplays can be tested in the future by combining precision measurements from the JUNO experiment with data from long

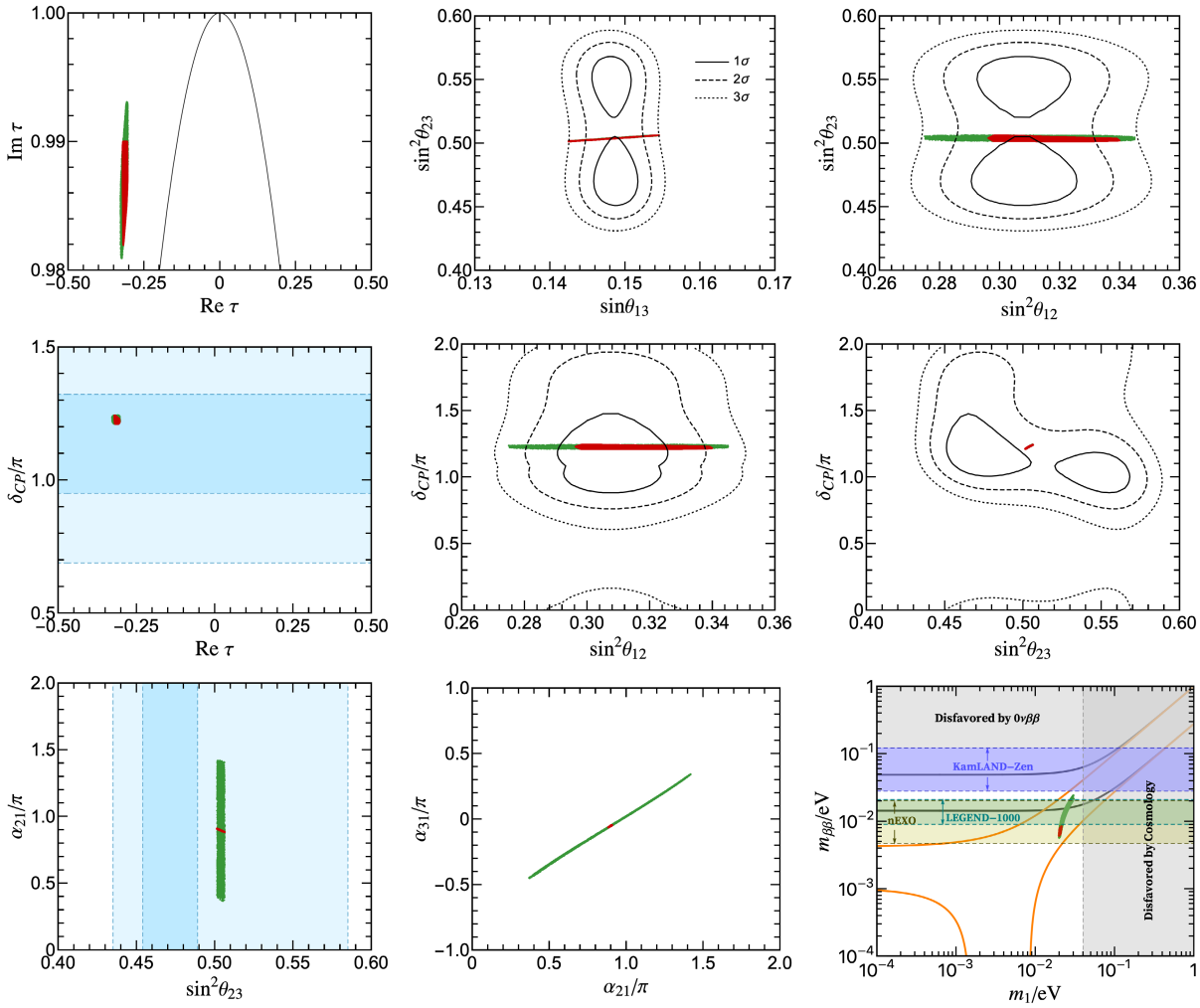

Fig. 6. (color online) Predicted correlations among the input parameters, lepton mixing angles, and CP-violating phases in the model $\{C_{10}^{(2,4,2)}, W_3\}$ with (red) and without (green) gCP symmetry for the NO neutrino mass spectrum.

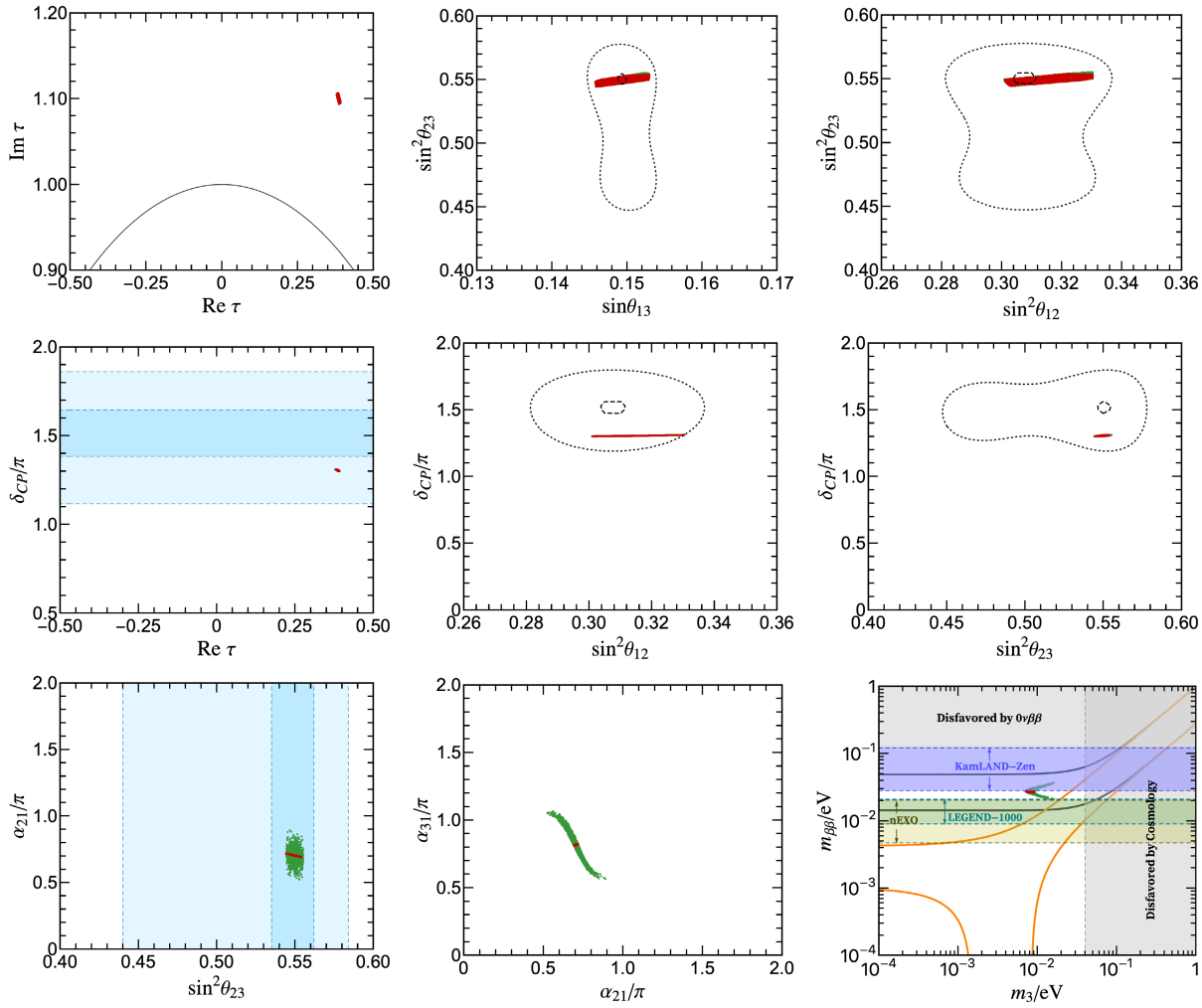

Fig. 7. (color online) Predicted correlations among the input parameters, lepton mixing angles, and CP-violating phases in the model $\{C_{10}^{(2,4,2)}, W_3\}$ with (red) and without (green) gCP symmetry for the IO neutrino mass spectrum.

baseline oscillation facilities such as DUNE or T2HK. In contrast, for our selected model, the total neutrino mass sum $\sum_{i=1}^{3} m_i$ and effective mass $m_{\beta\beta}$ do not show strong correlations with the mixing parameters; in particular, the degree of correlations is not comparable to that reported in Ref. [59], especially when the CP symmetry is not enforced.

IV. CONCLUSION

The modular invariance is a promising framework to describe the masses and mixing parameters of both quarks and leptons [13]. In the framework of original modular symmetry, SUSY is a necessary component. Thus, the principle of modular invariance forces the Yukawa couplings to be level N modular forms, which are holomorphic functions of the complex modulus τ. However, evidence for low-energy SUSY has not yet been reported. Subsequently, a non-supersymmetric formulation of the modular flavor symmetry was recently proposed in Refs. [33, 50]. This approach extends the standard level N modular forms by polyharmonic Maaß forms, a class of non-holomorphic modular forms that exist for zero, negative, and positive integer weights. The framework of non-holomorphic modular flavor symmetry presents a novel avenue for understanding the flavor structure of fermions.

In the present study, we perform a systematic analysis of all the minimal lepton models based on the non-holomorphic $\Gamma_3 \cong A_4$ modular symmetry. These models are explicitly constructed using only the modulus τ, with no additional flavon. In these models, light neutrino masses are generated by the effective Weinberg operator, whereas the Yukawa couplings are derived from polyharmonic Maaß forms of level 3 with even weights k in the range $-4 \leq k \leq 4$. The three LH lepton doublets transform as the A_4 triplet **3**, whereas the RH charged leptons $E^c_{1,2,3}$ are assigned to the A_4 singlets **1**, **1**′, or **1**″. According to the representation and weight assignments for the lepton fields, we have identified 1820 independent min-

imal models, each depending on eight real parameters: the six dimensionless inputs in Eq. (9) and two overall scales. When the non-holomorphic A_4 modular flavor symmetry is extended to combine with the gCP symmetry, one more free parameter are reduced for all these models. Numerically minimizing the χ^2 function for each model reveals 147 (six) phenomenologically viable models for the NO (IO) mass spectrum. Among these, only 47 (five) models remain consistent with the experimental data obtained from the lepton sector when gCP is imposed. The corresponding best fit values of the input parameters, lepton masses, lepton mixing angles, CP-violating phases, $0\nu\beta\beta$-decay effective Majorana mass, and kinematical mass are comprehensively presented in Tables 4, 5, 6, and 7. Based on our predictions, the current JUNO constraint on $\sin^2\theta_{12}$ rules out only five of the 147 viable NO models without gCP symmetry, whereas all the other models remain consistent with the experimental data. The future experimental results can significantly constrain the set of currently viable models. If the current best fit value of $\sin^2\theta_{12}$ remains unchanged, then JUNO will determine this parameter with high precision after six years of data accumulation. However, its projected 3σ interval still covers the $\sin^2\theta_{12}$ predictions of almost all the models considered in this study. The next-generation long baseline experiments such as DUNE and T2HK are projected to determine the atmospheric mixing angle θ_{23} with unprecedented precision, which will rule out a large fraction of the models. Additional constraints are expected from refined measurements of the Dirac CP-violating phase $\delta_{\rm CP}$, the sum of neutrino masses $\sum_{i=1}^{3} m_i$ and the effective Majorana mass $m_{\beta\beta}$ of $0\nu\beta\beta$-decay.

To illustrate our findings more clearly, we present detailed numerical results for the example model $\{C_{10}^{(2,4,2)}, W_3\}$, demonstrating the application of the non-holomorphic A_4 modular flavor symmetry to address the flavor problem. We present complete predictions for lepton mixing parameters, neutrino masses, and the effective mass of $0\nu\beta\beta$-decay under both NO and IO spectra, with and without gCP symmetry. Our analysis reveals several non-trivial correlations between the input parameters and physical observables for both the mass orderings. Furthermore, imposing gCP symmetry markedly reduces the allowed parameter space and yields significantly sharper, more definitive correlations. All these theoretical predictions can be rigorously tested by next-generation neutrino experiments. Notably, the specific predictions of this model will be verified in next-generation $0\nu\beta\beta$-decay experiments such as LEGEND-1000 and nEXO.

References

[1] S. Navas *et al.* (Particle Data Group Collaboration), Phys. Rev. D **110**(3), 030001 (2024)
[2] G. Altarelli and F. Feruglio, Rev. Mod. Phys. **82**, 2701 (2010), arXiv: 1002.0211[hep-ph]
[3] H. Ishimori, T. Kobayashi, H. Ohki *et al.*, Prog. Theor. Phys. Suppl. **183**, 1 (2010), arXiv: 1003.3552[hep-th]
[4] S. F. King and C. Luhn, Rept. Prog. Phys. **76**, 056201 (2013), arXiv: 1301.1340[hep-ph]
[5] S. F. King, A. Merle, S. Morisi *et al.*, New J. Phys. **16**, 045018 (2014), arXiv: 1402.4271[hep-ph]
[6] S. F. King, J. Phys. G **42**, 123001 (2015), arXiv: 1510.02091[hep-ph]
[7] S. F. King, Prog. Part. Nucl. Phys. **94**, 217 (2017), arXiv: 1701.04413[hep-ph]
[8] S. T. Petcov, Eur. Phys. J. C **78**(9), 709 (2018), arXiv: 1711.10806[hep-ph]
[9] Z. z. Xing, Phys. Rept. **854**, 1 (2020), arXiv: 1909.09610[hep-ph]
[10] F. Feruglio and A. Romanino, Rev. Mod. Phys. **93**(1), 015007 (2021), arXiv: 1912.06028[hep-ph]
[11] Y. Almumin, M. C. Chen, M. Cheng *et al.*, Universe **9**(12), 512 (2023), arXiv: 2204.08668[hep-ph]
[12] G. J. Ding and J. W. F. Valle, Phys. Rept. **1109**, 1 (2025), arXiv: 2402.16963[hep-ph]
[13] F. Feruglio, *Are neutrino masses modular forms?* pp. 227–266 (2019), arXiv: 1706.08749[hep-ph]
[14] T. Kobayashi and M. Tanimoto, Int. J. Mod. Phys. A **39**(09n10), 2441012 (2024), arXiv: 2307.03384[hep-ph]
[15] G. J. Ding and S. F. King, Rept. Prog. Phys. **87**(8), 084201 (2024), arXiv: 2311.09282[hep-ph]
[16] G. J. Ding, X. G. Liu, and C. Y. Yao, JHEP **01**, 125 (2023), arXiv: 2211.04546[hep-ph]
[17] G. J. Ding, X. G. Liu, J. N. Lu *et al.*, JHEP **11**, 083 (2023), arXiv: 2307.14926[hep-ph]
[18] G. J. Ding, E. Lisi, A. Marrone *et al.*, Phys. Rev. D **111**(7), 075024 (2025), arXiv: 2409.15823[hep-ph]
[19] M. C. Chen, S. Ramos-Sánchez, and M. Ratz, Phys. Lett. B **801**, 135153 (2020), arXiv: 1909.06910[hep-ph]
[20] A. Baur, H. P. Nilles, A. Trautner *et al.*, Phys. Lett. B **795**, 7 (2019), arXiv: 1901.03251[hep-th]
[21] A. Baur, H. P. Nilles, A. Trautner *et al.*, Nucl. Phys. B **947**, 114737 (2019), arXiv: 1908.00805[hep-th]
[22] H. P. Nilles, S. Ramos-Sánchez, and P. K. S. Vaudrevange, Phys. Lett. B **808**, 135615 (2020), arXiv: 2006.03059[hep-th]
[23] H. P. Nilles, S. Ramos-Sánchez, and P. K. S. Vaudrevange, Nucl. Phys. B **966**, 115367 (2021), arXiv: 2010.13798[hep-th]
[24] H. P. Nilles, S. Ramos-Sánchez, and P. K. S. Vaudrevange, JHEP **02**, 045 (2020), arXiv: 2001.01736[hep-ph]
[25] H. P. Nilles, S. Ramos-Sanchez, and P. K. S. Vaudrevange, Nucl. Phys. B **957**, 115098 (2020), arXiv: 2004.05200[hep-ph]
[26] G. J. Ding, S. F. King, C. C. Li *et al.*, JHEP **05**, 144 (2023), arXiv: 2303.02071[hep-ph]
[27] C. C. Li and G. J. Ding, JHEP **03**, 054 (2024), arXiv: 2308.16901[hep-ph]
[28] C. C. Li, J. N. Lu, and G. J. Ding, JHEP **12**, 015 (2024), arXiv: 2405.13460[hep-ph]
[29] M. C. Chen, V. Knapp-Perez, M. Ramos-Hamud *et al.*,

Phys. Lett. B **824**, 136843 (2022), arXiv: 2108.02240[hep-ph]
[30] J. Lauer, J. Mas, and H. P. Nilles, Phys. Lett. B **226**, 251 (1989)
[31] S. Ferrara, D. Lust, A. D. Shapere *et al*., Phys. Lett. B **225**, 363 (1989)
[32] S. Ferrara,. D. Lust, and S. Theisen, Phys. Lett. B **233**, 147 (1989)
[33] B. Y. Qu and G. J. Ding, JHEP **08**, 136 (2024), arXiv: 2406.02527[hep-ph]
[34] H. Okada and Y. Orikasa, *A radiative seesaw in a non-holomorphic modular S_3 flavor symmetry*, arXiv: 2501.15748[hep-ph]
[35] B. Kumar and M. K. Das, Int. J. Mod. Phys. A **40**(23), 2550090 (2025), arXiv: 2405.10586[hep-ph]
[36] T. Nomura and H. Okada, Phys. Lett. B **868**, 139763 (2025), arXiv: 2408.01143[hep-ph]
[37] T. Nomura and H. Okada, Phys. Lett. B **867**, 139618 (2025), arXiv: 2412.18095[hep-ph]
[38] T. Kobayashi, H. Okada, and Y. Orikasa, *Zee-Babu model in a non-holomorphic modular A_4 symmetry and modular stabilization*, arXiv: 2502.12662[hep-ph]
[39] M. A. Loualidi, M. Miskaoui, and S. Nasri, Phys. Rev. D **112**(1), 015008 (2025), arXiv: 2503.12594[hep-ph]
[40] B. Kumar and M. K. Das, JHEP **09**, 071 (2025), arXiv: 2504.21701[hep-ph]
[41] T. Nomura, H. Okada, and X. Y. Wang, JHEP **09**, 163 (2025), arXiv: 2504.21404[hep-ph]
[42] T. Nomura and H. Okada, *Neutrino mass model at a three-loop level from a non-holomorphic modular A_4 symmetry*, arXiv: 2506.02639[hep-ph]
[43] X. Zhang and Y. Reyimuaji, Phys. Rev. D **112**(7), 075050 (2025), arXiv: 2507.06945[hep-ph]
[44] Priya, L. Singh, B. C. Chauhan, and S. Verma, *Type-III Seesaw in Non-Holomorphic Modular Symmetry and Leptogenesis*, arXiv: 2508.05047[hep-ph]
[45] B. Kumar and M. K. Das, *Neutrino phenomenology and Dark matter in a left-right asymmetric model with non-holomorphic modular A_4 group*, arXiv: 2509.01205[hep-ph]
[46] S. K. Nanda, M. R. Devi, and S. Patra, *Non-Holomorphic A_4 Modular Symmetry in Type-I Seesaw: Implications for Neutrino Masses and Leptogenesis*, arXiv: 2509.22108[hep-ph]
[47] S. Jangid and H. Okada, *A radiative seesaw model in a non-invertible selection rule with the assistance of a non-holomorphic modular A_4 symmetry*, arXiv: 2510.17292[hep-ph]
[48] G. J. Ding, J. N. Lu, S. T. Petcov *et al*., JHEP **01**, 191 (2025), arXiv: 2408.15988[hep-ph]
[49] C. C. Li, J. N. Lu, and G. J. Ding, JHEP **12**, 189 (2024), arXiv: 2410.24103[hep-ph]
[50] B. Y. Qu, J. N. Lu, and G. J. Ding, *Non-holomorphic modular flavor symmetry and odd weight polyharmonic Maaß form*, arXiv: 2506.19822[hep-ph]
[51] C. C. Li and G. J. Ding, *Lepton models from non-holomorphic A_5' modular flavor symmetry*, arXiv: 2509.15183[hep-ph]
[52] P. P. Novichkov, J. T. Penedo, S. T. Petcov *et al*., JHEP **07**, 165 (2019), arXiv: 1905.11970[hep-ph]
[53] T. Dent, Phys. Rev. D **64**, 056005 (2001), arXiv: hep-ph/0105285
[54] T. Dent, JHEP **12**, 028 (2001), arXiv: hep-th/0111024
[55] A. Abusleme *et al.* (JUNO Collaboration), *First measurement of reactor neutrino oscillations at JUNO*, arXiv: 2511.14593[hep-ex]
[56] G. J. Ding, S. F. King, and X. G. Liu, JHEP **09**, 074 (2019), arXiv: 1907.11714[hep-ph]
[57] G. Altarelli and F. Feruglio, Nucl. Phys. B **741**, 215 (2006), arXiv: hep-ph/0512103
[58] I. Esteban, M. C. Gonzalez-Garcia, M. Maltoni *et al*., JHEP **12**, 216 (2024), arXiv: 2410.05380[hep-ph]
[59] P. P. Novichkov, J. T. Penedo, S. T. Petcov *et al*., JHEP **04**, 005 (2019), arXiv: 1811.04933[hep-ph]
[60] S. M. Bilenky, J. Hosek, and S. T. Petcov, Phys. Lett. B **94**, 495 (1980)
[61] N. Aghanim *et al.* (Planck Collaboration), Astron. Astrophys. **641**, A6 (2020) [Erratum: Astron. Astrophys. **652**, C4 (2021)], arXiv: 1807.06209[astro-ph.CO]
[62] I. Esteban, M. C. Gonzalez-Garcia, M. Maltoni *et al*., JHEP **09**, 178 (2020), arXiv: 2007.14792[hep-ph]
[63] A. Abusleme *et al*. JUNO Collaboration, Chin. Phys. C **46**(12), 123001 (2022), arXiv: 2204.13249[hep-ex]
[64] B. Abi *et al.* (DUNE Collaboration), *Deep Underground Neutrino Experiment (DUNE), Far Detector Technical Design Report, Volume II: DUNE Physics*, arXiv: 2002.03005[hep-ex]
[65] M. Archidiacono *et al*. (Euclid Collaboration), Astron. Astrophys. **693**, A58 (2025), arXiv: 2405.06047[astro-ph.CO]
[66] A. A. Esfahani *et al.* (Project 8 Collaboration), The Project 8 Neutrino Mass Experiment, in *Snowmass 2021*. 3, (2022), arXiv: 2203.07349[nucl-ex]
[67] S. Abe *et al.* (KamLAND-Zen Collaboration), *Search for Majorana Neutrinos with the Complete KamLAND-Zen Dataset*, arXiv: 2406.11438[hep-ex]
[68] N. Abgrall *et al.* (LEGEND Collaboration), *The Large Enriched Germanium Experiment for Neutrinoless $\beta\beta$ Decay: LEGEND-1000 Preconceptual Design Report*, arXiv: 2107.11462[physics.ins-det]
[69] G. Adhikari *et al*. (nEXO Collaboration), J. Phys. G **49**(1), 015104 (2022), arXiv: 2106.16243[nucl-ex]
[70] K. Abe *et al.* (Hyper-Kamiokande Collaboration), *Hyper-Kamiokande Design Report*, arXiv: 1805.04163[physics.ins-det]